

Matching next-to-leading-order and high-energy-resummed calculations of heavy-quarkonium-hadroproduction cross sections

Jean-Philippe Lansberg,^a Maxim Nefedov,^{1,a,b} Melih A. Ozelik^{a,c}

^a *Université Paris-Saclay, CNRS, IJCLab, 91405 Orsay, France*

^b *National Centre for Nuclear Research (NCBJ), Pasteura 7, 02-093 Warsaw, Poland*

^c *Institute for Theoretical Particle Physics, KIT, 76128 Karlsruhe, Germany*

E-mail: Jean-Philippe.Lansberg@in2p3.fr, maxim.nefedov@desy.de,
melih.oezcelik@kit.edu

ABSTRACT: The energy dependence of the total hadroproduction cross section of pseudo-scalar quarkonia is computed via matching Next-to-Leading Order (NLO) Collinear-Factorisation (CF) results with resummed higher-order corrections, proportional to $\alpha_s^n \ln^{n-1}(1/z)$, to the CF hard-scattering coefficient, where $z = M^2/\hat{s}$ with M and \hat{s} being the quarkonium mass and the partonic center-of-mass energy squared. The resummation is performed using High-Energy Factorisation (HEF) in the Doubly-Logarithmic (DL) approximation, which is a subset of the leading logarithmic $\ln(1/z)$ approximation. Doing so, one remains strictly consistent with the NLO and NNLO DGLAP evolution of the PDFs. By improving the treatment of the small- z asymptotics of the CF coefficient function, the resummation cures the unphysical results of the NLO CF calculation. The matching is directly performed in the z -space and, for the first time, by using the Inverse-Error Weighting (InEW) matching procedure. As a by-product of the calculation, the NNLO term of the CF hard-scattering coefficient proportional to $\alpha_s^2 \ln(1/z)$ is predicted from HEF.

¹Corresponding author.

Contents

1	Introduction: heavy-quarkonium cross-section instability at high energies	1
2	High-energy factorisation in the leading-logarithmic approximation	5
2.1	The resummed cross section in z -space	5
2.2	HEF coefficient functions	8
2.3	Resummation factor in the doubly-logarithmic approximation and beyond	10
2.4	Small- z hard-scattering coefficient at NLO and NNLO from resummation	13
2.5	Resummation by a μ_F choice	17
3	NLO+DLA matching in z-space	18
3.1	The subtractive-matching prescription	20
3.2	The inverse-error-weighting matching	20
4	Conclusions and outlook	25
A	Numerics in z-space	26
A.1	Method 1: regularised resummation factor	26
A.2	Method 2: small- q_T subtraction	27
B	Effects of the anomalous dimension beyond LO	29
C	Higher-twist effects	31

1 Introduction: heavy-quarkonium cross-section instability at high energies

Historically, the discovery of charm quarks and charmonia has been one of the most important milestones towards establishing QCD as the theory of strong interaction. Nowadays, charmonia and bottomonia attract a lot of attention as tools to study the proton structure, spin physics and/or to probe the quark-gluon plasma, see e.g. recent reviews [1–5]. They have clean experimental signatures and the fact that the hard scale of their production process is limited from below by the heavy-quark mass justifies the application of perturbation theory. However, the usage of quarkonia as tools for precision studies is problematic because up to now there is no consensus in the community on what are the main mechanisms of quarkonium production. The Non-Relativistic QCD(NRQCD) factorisation approach [6] at NLO in the α_s expansion and NNLO in the v^2 expansion, which seems to be the most systematic theoretical tool available so far, is able to describe the unpolarised p_T -differential hadroproduction cross sections of charmonia [7–13] and bottomonia [14–16].

However, this approach has essentially failed all other phenomenological tests. It is incapable [7–10] of describing the unpolarised photo- and hadroproduction data together with the data on quarkonium polarisation observables using a single set of Long-Distance Matrix Elements (LDMEs). This problem is known as the “polarisation puzzle”. Moreover, the hadroproduction of η_c at the LHC has unexpectedly turned out to be dominated by the color-singlet state $c\bar{c}[^1S_0^{[1]}]$, with no color-octet contribution needed to describe data [17]. This seems inconsistent with Heavy-quark spin symmetry relations between the LDMEs of η_c and J/ψ . This inconsistency is often referred to as the “heavy-quark-spin-symmetry puzzle”.

Alternative theoretical approaches, such as the (Improved) Colour-Evaporation Model [18–21] have their own phenomenological problems, e.g. being incapable to describe the J/ψ -pair hadroproduction [22], single J/ψ hadroproduction at large p_T [22] or $e^+e^- \rightarrow J/\psi + c + \bar{c}$ cross section [3]. Moreover, recent theoretical developments, such as potential-NRQCD [23] or soft-gluon factorisation [24–26] stay within the non-relativistic paradigm for the bound-state and try to either reduce number of free parameters in NRQCD or more accurately treat the kinematic effects of soft gluon emissions at hadronisation stage.

Given the situation described above, the logical way to proceed is to scrutinise all possible sources of numerically large higher-order corrections to the hard-scattering coefficient function in the NRQCD approach beyond fixed-order NLO in α_s computations and find possible ways to resum them to all orders in perturbation theory. For example, at high p_T , much larger than the quarkonium mass M , such a resummation has already been achieved via the fragmentation formalism which has been worked out up to the next-to-leading power in M/p_T [13, 27]. In the present paper, we focus on a class of higher-order QCD corrections, which has been largely ignored so far in the CF heavy-quarkonium-production literature and which become important when the hadronic collision energy, \sqrt{s} , is much larger than any other scale of our process, i.e. M or p_T .

For simplicity, we will focus on the case of the inclusive hadroproduction of the $^1S_0^{[1]}$, $^3P_0^{[1]}$ and $^3P_2^{[1]}$ NRQCD Fock states of a heavy-quark pair of mass M . These states can be produced at LO in CF via a $2 \rightarrow 1$ process, namely by fusion of two on-shell gluons. The NLO CF corrections to the total hadroproduction cross section at most involves $2 \rightarrow 2$ processes and can be computed in a closed form, which has been done long time ago [28, 29]. In CF, the total hadroproduction cross section of a state $m = ^{2S+1}L_J^{[1,8]}$ in a $h_A + h_B$ hadronic collision at a center-of-mass energy \sqrt{s} can be computed as a convolution:

$$\sigma^{[m],h_A h_B}(\sqrt{s}) = \sum_{i,j=q,\bar{q},g} \int_{z_{\min}}^1 \frac{dz}{z} \mathcal{L}_{ij}^{h_A h_B}(z, \mu_F) \hat{\sigma}_{ij}^{[m]}(z, \mu_F, \mu_R), \quad (1.1)$$

over the variable $z = M^2/\hat{s}$ which represents the squared fraction of the energy of the partons initiating the hard subprocess used to produce the observed final-state of mass M , with $z_{\min} = M^2/s$. The partonic luminosity for partons $i, j = q, \bar{q}, g$, entering eqn. (1.1) is:

$$\mathcal{L}_{ij}^{h_A h_B}(z, \mu_F) = \int_{-y_{\max}}^{+y_{\max}} dy \tilde{f}_i^{h_A} \left(\frac{M}{\sqrt{s}z} e^y, \mu_F \right) \tilde{f}_j^{h_B} \left(\frac{M}{\sqrt{s}z} e^{-y}, \mu_F \right), \quad (1.2)$$

where $y_{\max} = \ln \sqrt{s}z/M$ and¹ $\tilde{f}_i^h(x, \mu_F^2) = x f_i^h(x, \mu_F^2)$ are the collinear “momentum-density” PDFs of the parton i in a hadron h , evaluated at the factorisation scale μ_F . The quantity $\hat{\sigma}_{ij}^{[m]}$ in eqn. (1.1) is the hard-scattering coefficient for the corresponding partonic channel ij and state m .

The partonic luminosity is always decreasing when $z \rightarrow M^2/s$ corresponding to $y_{\max} \rightarrow 0$. However, at $\mu_F \gg 1$ GeV this decrease is more rapid than at $\mu_F \sim 1$ GeV, characteristic of quarkonium physics, due to μ_F -evolution of the x -dependence of PDFs in eqn. (1.2). It turns out that, at high scales, the contribution of small values of z to the integral (1.1) is suppressed by the partonic luminosity. However, at smaller scales $\mu_F \sim M \sim 1$ GeV most of the recent PDFs are relatively flat as functions of x , and the region of small z starts to significantly contribute to the cross section at high energies $\sqrt{s} \gg M$, see the detailed discussion in ref. [30]. For quarkonium-production cross sections at NLO in CF, the effect of the small- z region is dramatic, as it was understood already in refs. [31, 32].

For our forthcoming discussion, let us express the CF coefficient function from eqn. (1.1) as follows:

$$\hat{\sigma}_{ij}^{[m]} = \sigma_0^{[m]} \left[A_0^{[m]} \delta(1-z) + C_{ij} \frac{\alpha_s(\mu_R)}{\pi} \left(A_0^{[m]} \ln \frac{M^2}{\mu_F^2} + A_1^{[m]} \right) + \mathcal{O}(z\alpha_s, \alpha_s^2) \right], \quad (1.3)$$

where the first term in square brackets contributes only for the states $Q\bar{Q}[m]$ which can be produced in fusion of two on-shell gluons at $\mathcal{O}(\alpha_s^2)$. For such states, $A_0^{[m]} = 1$. For all the other $Q\bar{Q}[m]$ states, $A_0^{[m]} = 0$ so that $\hat{\sigma}_{ij}^{[m]}$ starts at $\mathcal{O}(\alpha_s^3)$. The second term in the square brackets of the eqn. (1.3) is the $z \rightarrow 0$ asymptotics of the $\mathcal{O}(\alpha_s^3)$ part of the coefficient function, while all the remaining terms are collected in the term $\mathcal{O}(\alpha_s z, \alpha_s^2)$. Overall factors $\sigma_0^{[m]}$ are defined in eqn. (2.12) below.

The Fock-state dependent constants $A_1^{[m]}$ in eqn. (1.3) are collected, for the cases when $A_0^{[m]} \neq 0$, in table 1 of ref. [30] and they turn out to be negative. The colour-factors C_{ij} in eqn. (1.3) are: $C_{gg} = 2C_A = 2N_c$, $C_{qg} = C_{gq} = C_F = (N_c^2 - 1)/(2N_c)$ and $C_{q\bar{q}} = 0$ (with $N_c = 3$ being the number of colours). If the series (1.3) is truncated at NLO in α_s , then for scale choices satisfying $\mu_F \geq M$, the contribution of the region $z \ll 1$ to the integral (1.1) becomes purely negative and, at sufficiently high energies, it may outweigh the positive NLO contribution from the $z \rightarrow 1$ limit and even the LO contribution.

For charmonium production characterised by $M \simeq 3$ GeV, this already happens at \sqrt{s} as modest as several hundreds of GeV [30, 32] making NLO calculation completely unpredictive at LHC energies. We find the problem described above very interesting because similar instabilities plague the energy-dependence of rapidity-differential cross sections of J/ψ hadroproduction in NRQCD factorisation at NLO [33] and could also affect the p_T -differential cross section at $p_T \lesssim M \ll \sqrt{s}$.

As it was realised in ref. [30], authored by two of us, these negative cross sections in CF at NLO stem from an *oversubtraction* of the collinear divergences inside the renormalised PDFs within the $\overline{\text{MS}}$ scheme. In principle, such a subtraction should be compensated by the evolution of the PDFs which progressively become steeper when μ_F increases. However, the

¹In what follows, we will omit h_A and h_B when referring to PDFs.

coefficients A_1 , which are related to the internal structure of the $gg \rightarrow Q\bar{Q}[m]$ form factor, are process-dependent as opposed to the PDF evolution governed by the Dokshitzer-Gribov-Lipatov-Altarelli-Parisi (DGLAP) [34–36] equations. As such, the negative numbers cannot be systematically compensated by the PDF evolution. This mismatch between the partonic cross section and the PDFs is most dramatic for low scale processes for which the PDFs are the flattest.

The small- z behaviour of the NLO partonic cross section of the type (1.3) is characteristic of many hard processes, as it was shown for the first time in ref. [37] for the cases of total open heavy-flavour hadro- and photoproduction as well as prompt-photon hadroproduction. In these cases, the coefficients A_1 turn out to be positive, whereas they are negative for the hadroproduction of 1S_0 , 3P_0 and 3P_2 -states of heavy quark–anti-quark pairs as mentioned above, as well as for the photoproduction of 3S_1 [38]. For Higgs-boson hadroproduction, the sign of the coefficient A_1 depends on the ratio M_{H^0}/m_t (see ref. [30]). These observations clearly point at the fact that it is impossible to absorb the impact of A_1 into the PDFs via the global scheme redefinition proposed in ref. [37]: the optimal subtraction scheme for the open heavy-flavour hadroproduction will be worse than $\overline{\text{MS}}$ for heavy quarkonia at high energies, and vice-versa.

In ref. [30], two of us have proposed a new scale prescription for the factorisation scale to cure the mismatch between the partonic cross section and the PDF evolution (for processes with $A_0 = 1$):

$$\hat{\mu}_F = M \exp \left[A_1^{[m]}/2 \right], \quad (1.4)$$

which restores the positivity of quarkonium-production cross sections (see refs. [30, 38]). As it will be explained in section 2.5, this scale choice corresponds to an attempt to resum some higher-order QCD corrections proportional to:

$$\alpha_s^n \ln^{n-1} \frac{1}{z}, \quad (1.5)$$

at leading power in z for $z \ll 1$ within $\hat{\sigma}_{ij}$. In what follows, we will refer to the all order in α_s resummation of the contributions of the type (1.5) as the *Leading Logarithmic*- $\ln(1/z)$ *Approximation* or $\text{LL}(\ln(1/z))$ for short. The advantage of the $\hat{\mu}_F$ -prescription in comparison to the global scheme redefinition is that it is process-dependent, i.e. every process is evaluated with its own scale (1.4).

However, beyond $\mathcal{O}(\alpha_s)$, the approximate resummation via the $\hat{\mu}_F$ -prescription does not correctly capture the structure of QCD corrections of the type (1.5). For instance, as we will see, the $\alpha_s^2 \ln 1/z$ coefficient of the expanded expression of the NLO cross section obtained with $\mu_F = \hat{\mu}_F$ does not correspond to the one obtained from the resummation formalism. The systematic formalism for such a resummation requires the use of the Balitsky-Fadin-Kuraev-Lipatov (BFKL) evolution [39–41] of the partonic amplitude in the rapidity $Y \sim \ln(1/z) \gg 1$ with its non-trivial transverse-momentum dynamics to correctly capture higher-order QCD corrections even in the $\text{LL}(\ln(1/z))$ approximation. Such a formalism is known as *High Energy Factorisation (HEF)* and has been developed in refs. [42–45] in the $\text{LL}(\ln(1/z))$ approximation. In the past, this formalism has been successfully applied to study the high-energy structure of hard-scattering coefficients of CF for many processes,

such as Higgs [46, 47], Drell-Yan lepton-pair [48] and prompt-photon production [49]. In particular, in ref. [48] the correctness of the resummation predictions up to NNLO in α_s has been verified. Recently, the NLL($\ln(1/z)$) resummation for lepton-hadron Deep-Inelastic Scattering has been shown to significantly improve the quality of NNLO PDF fits [50, 51].

With the present paper, we fill the gap in the existing HEF literature, providing the first NLO CF + LL($\ln(1/z)$) matched calculation of the energy-dependence of the total heavy-quarkonium-hadroproduction cross section. The aforementioned HEF calculations [46–49] use the representation of the resummed cross section in Mellin space, which is convenient from the computational point of view, but is difficult to match with NLO CF results. We therefore perform a matching between the HEF-resummed hard-scattering coefficient, which is valid at $z \ll 1$, and the full NLO CF correction, which contains numerically important $\mathcal{O}(z)$ power corrections, directly in z -space. Along the same lines as in ref. [52], we propose a new matching procedure, described in section 3.2, which smoothly interpolates between $z \rightarrow 0$ and $z \rightarrow 1$ limits.

The paper has the following structure. In section 2, we describe the LL($\ln(1/z)$) HEF formalism, in particular the structure of the resummed partonic cross section in z -space (section 2.1), the corresponding process-dependent coefficient functions (section 2.2) and universal resummation factors (section 2.3). In section 2.4, we expand the resummed cross section up to NNLO in α_s to verify its consistency with NLO results [28, 29] and provide predictions for future NNLO calculations of quarkonium production cross section. In section 2.5, we explain the relation of the HEF formalism with the $\hat{\mu}_F$ scale prescription. In section 3, we introduce two matching procedures in z -space, compare the corresponding numerical results and discuss the uncertainties of our calculation. Finally, in section 4, we summarise our conclusions and prospects for future studies. The paper contains three appendices: in appendix A, we explain two methods which we have developed to calculate the resummed cross section in z -space in a numerically-stable way. In appendix B, we show the numerical effects of the $\mathcal{O}(\alpha_s^2)$ corrections to the anomalous dimension (2.20) on the μ_F dependence of the resummed part of the cross section and, in appendix C, we discuss the possible size of non-perturbative effects, due to the intrinsic transverse momentum of gluons in the proton, on the value of the total quarkonium production cross section in our approximation.

2 High-energy factorisation in the leading-logarithmic approximation

2.1 The resummed cross section in z -space

Considering the qg channel as an example, the corrections proportional to $\alpha_s^n \ln^{n-1} 1/z$ to the QCD hard subprocess for the production of the final-state of interest, $Q\bar{Q}[m]$, with a four-momentum p come from processes with at most n additional partons in the final state:

$$g(p_1) + q(p_2) \rightarrow g(k_1) + g(k_2) + \dots + Q\bar{Q}[m](p) + \dots + g(k_{n-1}) + q(k_n), \quad (2.1)$$

where the four-momentum labels are given in parentheses.

At leading-power in z and in the LL($\ln(1/z)$) approximation, only the final states with a strong ordering in the corresponding light-cone components of momenta contribute, that

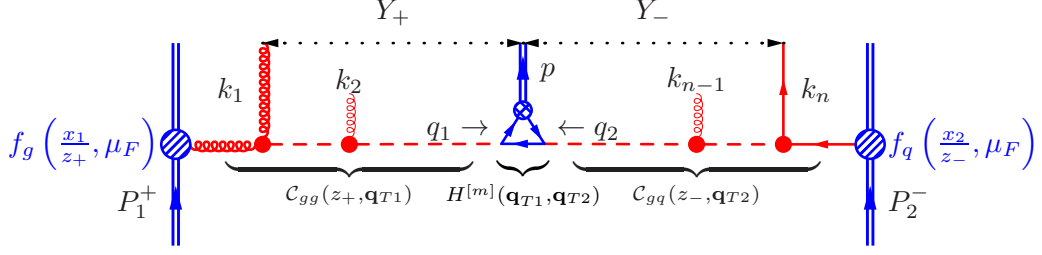


Figure 1. Typical diagrams contributing to the high-energy factorisation amplitude in the gg -channel. The dashed lines denote Reggeised gluon exchanges, while solid circles denote Lipatov’s vertices.

is when:

$$p_1^+ \simeq k_1^+ \gg k_2^+ \gg \dots \gg p^+ \gg \dots \gg k_{n-1}^+ \gg k_n^+,$$

$$k_1^- \ll k_2^- \ll \dots \ll p^- \ll \dots \ll k_{n-1}^- \ll k_n^- \simeq p_2^-,$$

where $k_i^\pm = k_i^0 \pm k_i^3$, so that, for the four-momenta of the incoming protons, one has $P_1^+ = \sqrt{s}$, $P_1^- = 0$ and $P_2^+ = 0$, $P_2^- = \sqrt{s}$. This limit is referred to as the *Multi-Regge Kinematics (MRK)*. In this limit and at this accuracy, the QCD amplitudes are known to factorise into a product of gauge-invariant blocks: the Lipatov’s scattering, the production vertices [39–41], the t -channel Reggeised gluon propagators and the effective vertex for production of the $Q\bar{Q}[m]$ state, see the figure 1. For a review, the reader can consult the monographs [53, 54] or the lecture notes [55]. This factorisation at the amplitude level allows one to factorise out the corresponding cross-section-level blocks: the universal *resummation factors* \mathcal{C}_{gi} , with $i = g, q, \bar{q}$, and the process-dependent *coefficient function* $H^{[m]}$.

The resummation factors are solutions of the BFKL equation, describing the rapidity-evolution of the cascade of emissions from the rapidities of the most backward/forward partons in the hard process to the rapidity of the observed final state. The corresponding rapidity intervals (figure 1) can be estimated in the MRK as:

$$Y_+ = \frac{1}{2} \left(\ln \frac{k_1^+}{k_1^-} - \ln \frac{p^+}{p^-} \right) \simeq \ln \left[\frac{p_1^+}{p_+} \frac{M_T}{|\mathbf{k}_{T1}|} \right] = \ln \frac{1}{z_+} + \ln \frac{M_T}{|\mathbf{k}_{T1}|}, \quad (2.2)$$

$$Y_- = \frac{1}{2} \left(\ln \frac{p^+}{p^-} - \ln \frac{k_n^+}{k_n^-} \right) \simeq \ln \left[\frac{p_2^-}{p_-} \frac{M_T}{|\mathbf{k}_{Tn}|} \right] = \ln \frac{1}{z_-} + \ln \frac{M_T}{|\mathbf{k}_{Tn}|}, \quad (2.3)$$

where $M_T^2 = M^2 + \mathbf{p}_T^2$, $z_+ = p_+/p_1^+$ and $z_- = p_-/p_2^-$ are fractions of (+/-) light-cone components entering the hard process, which are used up to produce the final state $Q\bar{Q}[m]$. In terms of z_+ and z_- , the “global” z variable introduced above is equal to:

$$z = \frac{M^2}{\hat{s}} = \frac{M^2}{p_1^+ p_2^-} = \frac{M^2}{M_T^2} z_+ z_-. \quad (2.4)$$

The LL BFKL evolution of the resummation factors \mathcal{C}_{gi} in rapidity resums higher-order corrections to the cross section proportional to $\alpha_s^n Y_\pm^{n-1}$. If one is only interested in

the resummation of the $\ln 1/z$ -corrections in the $\text{LL}(\ln(1/z))$ approximation, as we do in the present paper, then one solves the BFKL equation for resummation factors, neglecting transverse-momentum logarithms in eqns. (2.2) and (2.3), i.e. putting $Y_{\pm} \simeq \ln 1/z_{\pm}$, as it has been done in the seminal papers [42–45].

If the transverse-momentum logarithms in eqns. (2.2) and (2.3) are not neglected, then in addition to $\ln 1/z$ -corrections the HEF actually resums the LL $\alpha_s^n \ln^{2n}(|\mathbf{p}_T|/M)$ and part of the NLL $\alpha_s^n \ln^n(|\mathbf{p}_T|/M)$ corrections, which are traditionally considered within the framework of Transverse-Momentum Dependent (TMD) factorisation [56]. This overlap between TMD and High-Energy factorisations has been explored in recent papers [57, 58].

Postponing a more detailed discussion of the resummation factors until section 2.3, let us write down the factorisation formula for the rapidity-differential cross section in HEF:

$$\begin{aligned} \frac{d\sigma}{dy} = & \sum_{i,j=g,q,\bar{q}} \int_0^{\infty} d\mathbf{q}_{T1}^2 d\mathbf{q}_{T2}^2 \int_{x_1}^1 \frac{dz_+}{z_+} \tilde{f}_i\left(\frac{x_1}{z_+}, \mu_F\right) \mathcal{C}_{gi}(z_+, \mathbf{q}_{T1}^2, \mu_F, \mu_R) \\ & \times \int_{x_2}^1 \frac{dz_-}{z_-} \tilde{f}_j\left(\frac{x_2}{z_-}, \mu_F\right) \mathcal{C}_{gj}(z_-, \mathbf{q}_{T2}^2, \mu_F, \mu_R) \int_0^{2\pi} \frac{d\phi}{2} \frac{H^{[m]}(\mathbf{q}_{T1}^2, \mathbf{q}_{T2}^2, \phi)}{M_T^4}, \end{aligned} \quad (2.5)$$

where $x_1 = M_T e^y / \sqrt{s}$ and $x_2 = M_T e^{-y} / \sqrt{s}$ with $M_T^2 = M^2 + (\mathbf{q}_{T1} + \mathbf{q}_{T2})^2$ and ϕ being the azimuthal angle between \mathbf{q}_{T1} and \mathbf{q}_{T2} . The HEF coefficient function $H^{[m]}$ non-trivially depends on the transverse momenta $\mathbf{q}_{T1,2}$ of the Reggeised gluons entering it (figure 1), and the procedure for its computation is described in section 2.2. As it will become clear below, this transverse-momentum dependence is the key to the factorisation of higher-order terms enhanced by $\ln 1/z$ in the QCD perturbative series in terms of the process-independent resummation functions \mathcal{C}_{gj} , encapsulating logarithms $\ln 1/z_{\pm}$ and the process dependent coefficients $H^{[m]}$, which are free from these large logarithms.

Integrating eqn. (2.5) over the rapidity and introducing the variables $\eta = \ln(z_+/z_-)/2$ and z via eqn. (2.4), one can recast the total hadronic cross section in HEF into the form of eqn. (1.1) with the partonic coefficient:

$$\begin{aligned} \hat{\sigma}_{ij}^{[m], \text{HEF}}(z, \mu_F, \mu_R) = & \int_{-\infty}^{\infty} d\eta \int_0^{\infty} d\mathbf{q}_{T1}^2 d\mathbf{q}_{T2}^2 \mathcal{C}_{gi}\left(\frac{M_T}{M} \sqrt{z} e^{\eta}, \mathbf{q}_{T1}^2, \mu_F, \mu_R\right) \\ & \times \mathcal{C}_{gj}\left(\frac{M_T}{M} \sqrt{z} e^{-\eta}, \mathbf{q}_{T2}^2, \mu_F, \mu_R\right) \int_0^{2\pi} \frac{d\phi}{2} \frac{H^{[m]}(\mathbf{q}_{T1}^2, \mathbf{q}_{T2}^2, \phi)}{M_T^4}, \end{aligned} \quad (2.6)$$

where the integration over η actually proceeds only over $|\eta| \leq \eta_{\text{max}} = \ln[M/(M_T \sqrt{z})]$, because the arguments of the resummation functions z_{\pm} should be smaller or equal than one.

Finally let us emphasise that, for the gg channel, the transverse-momentum integrals in eqn. (2.6) can not be dealt with numerically unless the LO contribution $\sigma_0^{[m]} \delta(1-z)$ is explicitly removed from eqn. (2.6):

$$\hat{\sigma}_{gg}^{[m], \text{HEF}}(z, \mu_F, \mu_R) = \sigma_0^{[m]} \delta(1-z) + \check{\sigma}_{gg}^{[m], \text{HEF}}(z, \mu_F, \mu_R), \quad (2.7)$$

where $\check{\sigma}_{gg}^{[m], \text{HEF}}$ is the LO-*subtracted* resummed hard-scattering coefficient. The LO CF contribution is contained in the $\hat{\sigma}_{gg}^{[m], \text{HEF}}$ because the perturbative expansion for resummation factors \mathcal{C}_{gg} starts with the LO term $\delta(1-z)\delta(\mathbf{q}_T^2)$, which corresponds to the case with no additional emissions. The procedure (2.7) turns the integrals in eqn. (2.6) into well-defined functions of z . We describe two methods which we have used to isolate the LO contribution in the Appendix A. The method of the section A.1 relies on the form of resummation factor in the Doubly-Logarithmic approximation, which we will introduce in eqn. (2.30) in section 2.3, while the method in section A.2 is more general and is applicable to the exact LL($\ln(1/z)$) resummation factor (2.18) and its generalisations.

2.2 HEF coefficient functions

For the following $2 \rightarrow 1$ processes:

$$R(q_1) + R(q_2) \rightarrow c\bar{c} \left[{}^1S_0^{[1,8]}, {}^3S_1^{[8]}, {}^3P_{0,1,2}^{[1,8]} \right], \quad (2.8)$$

the corresponding HEF coefficient functions are non-zero at LO in α_s . In eqn. (2.8), the incoming Reggeised gluons are denoted by the symbol R and their four-momenta can be parametrised as $q_1^\mu = x_1 P_1^\mu + q_{T1}^\mu$ and $q_2^\mu = x_2 P_2^\mu + q_{T2}^\mu$ (figure 1) so that $q_{1,2}^2 = -\mathbf{q}_{T1,2}^2 < 0$. The Feynman rules of Lipatov's gauge-invariant EFT for Multi-Regge processes in QCD [59] are used for the computation of HEF coefficient functions for general QCD processes, as it was done for quarkonia in Ref. [60]. The use of the High-Energy EFT is particularly important for the gauge invariance² of the computation of the coefficient function for production of the ${}^3S_1^{[8]}$ -state. Essentially, the Lipatov's vertex should be used instead of the usual three-gluon vertex.³

In the present paper we take the explicit expressions for HEF coefficient functions, which can be directly plugged into our eqn. (2.6), from ref. [64]. The HEF coefficient functions satisfy the on-shell-limit normalisation condition:

$$\int_0^{2\pi} \frac{d\phi}{2\pi} \lim_{\mathbf{q}_{T1,2}^2 \rightarrow 0} H^{[m]}(\mathbf{q}_{T1}^2, \mathbf{q}_{T2}^2, \phi) = \frac{1}{4(N_c^2 - 1)^2} \sum_{\lambda_{1,2}=\pm} \left| \mathcal{M}(g_{\lambda_1} g_{\lambda_2} \rightarrow Q\bar{Q}[m]) \right|^2, \quad (2.10)$$

with the corresponding CF squared amplitude \mathcal{M} averaged over colours and helicities $\lambda_{1,2}$ of the initial-state gluons. It is convenient to separate out the corresponding colour

²With respect to gauge choice of internal gluon propagator.

³Indeed, for the states listed in eqn. (2.8), except for ${}^3S_1^{[8]}$, the EFT computation is equivalent to the use of the following ‘‘nonsense’’ polarisation prescription for the initial-state gluons:

$$\varepsilon^\mu(q_{1,2}) \rightarrow \frac{q_{T1,2}^\mu}{|\mathbf{q}_{T1,2}|}, \quad (2.9)$$

due to Slavnov-Taylor identities of QCD. However, for more complicated processes containing final-state gluons coupling to initial-state ones, or otherwise essentially non-Abelian, as e.g. double color-octet channels in heavy-quarkonium pair production [61], the full set of Feynman rules of the EFT [59] have to be used instead of the prescription (2.9). The coefficient functions for the processes (2.8) have been computed for the first time in [62–64] using the prescription (2.9) and later have been reproduced in the ref. [60] using Lipatov's EFT.

factors, the LDMEs of NRQCD $\langle \mathcal{O}[m] \rangle$ and the CF spin-orbital factors from the coefficient functions as follows:

$$H^{[m]}(\mathbf{q}_{T1}^2, \mathbf{q}_{T2}^2, \phi) = \frac{M^4 \sigma_0^{[m]}}{\pi} F^{[m]}(\mathbf{q}_{T1}^2, \mathbf{q}_{T2}^2, \phi), \quad (2.11)$$

where the $\sigma_0^{[m]}$ factors are:

$$\begin{aligned} \sigma_0^{[1S_0^{[1]}]} &= \frac{2}{9} \pi^3 \alpha_s^2 \frac{\langle \mathcal{O}[1S_0^{[1]}] \rangle}{M^5}, \\ \sigma_0^{[1S_0^{[8]}]} &= \frac{5}{12} \pi^3 \alpha_s^2 \frac{\langle \mathcal{O}[1S_0^{[8]}] \rangle}{M^5}, \\ \sigma_0^{[3S_1^{[8]}]} &= \frac{1}{2} \pi^3 \alpha_s^2 \frac{\langle \mathcal{O}[3S_1^{[8]}] \rangle}{M^5}, \\ \sigma_0^{[3P_0^{[1]}]} &= \frac{8}{3} \pi^3 \alpha_s^2 \frac{\langle \mathcal{O}[3P_0^{[1]}] \rangle}{M^5}, \\ \sigma_0^{[3P_1^{[1]}]} &= \frac{16}{3} \pi^3 \alpha_s^2 \frac{\langle \mathcal{O}[3P_1^{[1]}] \rangle}{M^7}, \\ \sigma_0^{[3P_2^{[1]}]} &= \frac{32}{45} \pi^3 \alpha_s^2 \frac{\langle \mathcal{O}[3P_2^{[1]}] \rangle}{M^7}, \\ \sigma_0^{[3P_0^{[8]}]} &= 5 \pi^3 \alpha_s^2 \frac{\langle \mathcal{O}[3P_0^{[8]}] \rangle}{M^7}, \\ \sigma_0^{[3P_1^{[8]}]} &= 10 \pi^3 \alpha_s^2 \frac{\langle \mathcal{O}[3P_1^{[8]}] \rangle}{M^7}, \\ \sigma_0^{[3P_2^{[8]}]} &= \frac{4}{3} \pi^3 \alpha_s^2 \frac{\langle \mathcal{O}[3P_2^{[8]}] \rangle}{M^7}. \end{aligned} \quad (2.12)$$

The functions $F^{[m]}$ in the eqn. (2.11) do not depend on the colour state of the $Q\bar{Q}$ pair and depend only on its spin and orbital momentum. For the S -states they are:

$$F^{[1S_0]}(t_1, t_2, \phi) = 2 \frac{(M^2 + \mathbf{p}_T^2)^2}{(M^2 + t_1 + t_2)^2} \sin^2 \phi, \quad (2.13)$$

$$F^{[3S_1]}(t_1, t_2, \phi) = \frac{(M^2 + \mathbf{p}_T^2) [(t_1 + t_2)^2 + M^2 (t_1 + t_2 - 2\sqrt{t_1 t_2} \cos \phi)]}{M^2 (M^2 + t_1 + t_2)^2}, \quad (2.14)$$

with $\mathbf{p}_T^2 = (\mathbf{q}_{T1} + \mathbf{q}_{T2})^2 = t_1 + t_2 + 2\sqrt{t_1 t_2} \cos \phi$ with $t_{1,2} = \mathbf{q}_{T1,2}^2$. For the P -wave states, one has:

$$\begin{aligned} F^{[3P_0]}(t_1, t_2, \phi) &= \frac{2}{9} \frac{(M^2 + \mathbf{p}_T^2)^2 [(3M^2 + t_1 + t_2) \cos \phi + 2\sqrt{t_1 t_2}]^2}{(M^2 + t_1 + t_2)^4}, \\ F^{[3P_1]}(t_1, t_2, \phi) &= \frac{2}{9} \frac{(M^2 + \mathbf{p}_T^2)^2 [(t_1 + t_2)^2 \sin^2 \phi + M^2 (t_1 + t_2 - 2\sqrt{t_1 t_2} \cos \phi)]}{(M^2 + t_1 + t_2)^4}, \\ F^{[3P_2]}(t_1, t_2, \phi) &= \frac{1}{3} \frac{(M^2 + \mathbf{p}_T^2)^2}{(M^2 + t_1 + t_2)^4} \left\{ 3M^4 + 3M^2(t_1 + t_2) + 4t_1 t_2 \right. \\ &\quad \left. + (t_1 + t_2)^2 \cos^2 \phi + 2\sqrt{t_1 t_2} [3M^2 + 2(t_1 + t_2)] \cos \phi \right\}. \end{aligned} \quad (2.15)$$

The on-shell limits (2.10) of the functions $F^{[m]}$ are equal to one or zero, depending on whether the corresponding state is allowed to be produced in a fusion of two on-shell gluons by the Landau-Yang theorem, i.e. they are equal to constants A_0 first introduced in eqn. (1.3).

2.3 Resummation factor in the doubly-logarithmic approximation and beyond

Following the original refs. [42–45], we introduce the Mellin transform with respect to the z -dependence of the resummation factor as follows:

$$\mathcal{C}(N, \mathbf{q}_T, \mu_F, \mu_R) = \int_0^1 dz z^{N-1} \mathcal{C}(z, \mathbf{q}_T, \mu_F, \mu_R), \quad (2.16)$$

so that the logarithms which we aim to resum are mapped to poles at $N = 0$ in Mellin space:

$$\ln^{k-1} \frac{1}{z} \leftrightarrow \frac{(k-1)!}{N^k}. \quad (2.17)$$

The emissions of additional partons at higher orders in α_s generate collinear divergences in the resummation factor which have been removed in ref. [44] using a transverse-momentum cut off and using dimensional regularisation and the $\overline{\text{MS}}$ -subtraction prescription in ref. [45]. After the subtraction of the collinear divergences, the dependence on factorisation scale μ_F arises in the resummation factor. The Mellin-space result [42–45] for the subtracted resummation factor is:

$$\mathcal{C}_{gg}(N, \mathbf{q}_T^2, \mu_F, \mu_R) = R(\gamma_{gg}(N, \alpha_s)) \frac{\gamma_{gg}(N, \alpha_s)}{\mathbf{q}_T^2} \left(\frac{\mathbf{q}_T^2}{\mu_F^2} \right)^{\gamma_{gg}(N, \alpha_s)}, \quad (2.18)$$

where $\hat{\alpha}_s = \alpha_s(\mu_R) C_A / \pi$. The choice of the scale at which the α_s is evaluated in the \mathcal{C}_{gg} function is not strictly dictated by the LL($\ln(1/z)$) resummation or NLO CF results. However, since both \mathcal{C}_{gg} functions and HEF coefficient function belong to the coefficient function of CF $\hat{\sigma}_{ij}^{[m]}$ (see eqn. (2.6)), we opt to choose the same scale μ_R of the α_s in all these quantities. The anomalous dimension γ_{gg} is the solution of the algebraic equation first derived in the ref. [65]:

$$\frac{\hat{\alpha}_s}{N} \chi(\gamma_{gg}(N, \alpha_s)) = 1, \quad (2.19)$$

where $\chi(\gamma) = 2\psi_0(1) - \psi_0(\gamma) - \psi_0(1 - \gamma)$ is the Lipatov's LO characteristic function and $\psi_n(\gamma) = d^n \ln \Gamma(\gamma) / d\gamma^n$ is the Euler's ψ function. The first few terms of the perturbative solution of eqn. (2.19) are:

$$\gamma_{gg}(N, \alpha_s) = \gamma_N + 2\zeta(3) \frac{\hat{\alpha}_s^4(\mu_R)}{N^4} + 2\zeta(5) \frac{\hat{\alpha}_s^6(\mu_R)}{N^6} + \mathcal{O}(\alpha_s^7), \quad \text{where } \gamma_N = \frac{\hat{\alpha}_s(\mu_R)}{N}. \quad (2.20)$$

Eqn. (2.18) and the anomalous dimension (2.20) resum the series of higher-order corrections proportional to α_s^n / N^n . These corrections by virtue of the mapping (2.17) are equivalent to the LL($\ln(1/z)$)-approximation (1.5). While the LL($\ln(1/z)$) anomalous dimension (2.20) is scheme-independent in a wide class of $\overline{\text{MS}}$ -like schemes [45], the factor

$R(\gamma)$ encapsulates the subtraction-scheme dependence. For the $\overline{\text{MS}}$ scheme, its perturbative expansion starts at N³LO [45, 66]:

$$R(\gamma_{gg}(N, \alpha_s)) = 1 + \mathcal{O}(\alpha_s^3). \quad (2.21)$$

Let us now define the resummation factors for the quark-induced channels. As depicted in figure 1, in the LL(ln(1/z))-approximation, only Reggeised gluons can propagate in the t -channel. Hence, the quarks can only participate in so-called LO *partonic impact factors*. The corresponding expression for the squared amplitude in the LL(ln(1/z)) approximation differs from the similar squared amplitude with gluon substituted by the quark only by an overall colour factor. This picture leads to the simple relation between the quark and gluon-induced resummation factors in the LL(ln(1/z)) approximation:

$$\mathcal{C}_{gq}(z, \mathbf{q}_T^2, \mu_F, \mu_R) = \frac{C_F}{C_A} \left[\mathcal{C}_{gg}(z, \mathbf{q}_T^2, \mu_F, \mu_R) - \delta(1-z)\delta(\mathbf{q}_T^2) \right], \quad (2.22)$$

where the subtraction term in square brackets removes the contribution of the direct $g \rightarrow R$ transition in the on-shell limit. The latter is absent in case of quarks due to the fermion-number conservation.

To clarify the physical meaning of the anomalous dimension γ_{gg} in eqn. (2.18), let us observe that, since the Mellin transform turns z_{\pm} -convolutions in eqn. (2.5) into products, the μ_F independence of the cross section order by order in α_s is achieved provided that:

$$\sum_{i=q, \bar{q}, g} \frac{\partial}{\partial \ln \mu_F^2} \left[\tilde{f}_i(N, \mu_F) \mathcal{C}_{gi}(N, \mathbf{q}_T^2, \mu_F, \mu_R) \right] = 0, \quad (2.23)$$

at any \mathbf{q}_T . Substituting eqns. (2.18) and (2.22) one finds that eqn. (2.23) is indeed satisfied due to the following form of DGLAP equations at LL(ln 1/z) accuracy:

$$\frac{\partial \tilde{f}_g(N, \mu_F)}{\partial \ln \mu_F^2} = \gamma_{gg}(N, \alpha_s) \left[\tilde{f}_g(N, \mu_F) + \frac{C_F}{C_A} \sum_{i=q, \bar{q}} \tilde{f}_i(N, \mu_F) \right], \quad (2.24)$$

$$\frac{\partial \tilde{f}_q(N, \mu_F)}{\partial \ln \mu_F^2} = 0. \quad (2.25)$$

In other words, the $\gamma_{gg}(N, \alpha_s)$ is the LL(ln(1/z)) approximation to the anomalous dimension of the DGLAP equations, governing the scale dependence of the gluon momentum density distribution, while $C_F \gamma_{gg}/C_A$ determines the feed down from quarks to gluon in this approximation. Indeed, the corresponding LO DGLAP splitting functions have the following $z \rightarrow 0$ asymptotics:

$$\frac{\alpha_s}{2\pi} z P_{gg}(z) = \hat{\alpha}_s + \mathcal{O}(z), \quad (2.26)$$

$$\frac{\alpha_s}{2\pi} z P_{gq}(z) = \frac{C_F}{C_A} \hat{\alpha}_s + \mathcal{O}(z). \quad (2.27)$$

Eqn. (2.26) is equivalent to the first term of the solution (2.20) via the mapping (2.17), while eqn. (2.27) is related in the same way to the first term of the expansion of $C_F \gamma_{gg}/C_A$

in α_s . The coefficients in front of $\alpha_s \ln(1/z)$ and $\alpha_s^2 \ln^2(1/z)$ terms in the NLO and NNLO contributions to $zP_{gg}(z)$ are zero in QCD, consistently with eqn. (2.20). The first non-zero contributions at leading power in z beyond LO in α_s in QCD are $\mathcal{O}(\alpha_s^2)$ and $\mathcal{O}(\alpha_s^3 \ln(1/z))$. They belong to the NLL($\ln(1/z)$) approximation and their consistency with NLL($\ln(1/z)$) BFKL predictions has been verified in ref. [67], while the consistency of the LL($\ln(1/z)$) series (2.20) with the DGLAP anomalous dimension in $\mathcal{N} = 4$ -supersymmetric Yang-Mills theory in the large- N_c limit has been checked in ref. [68] up to five loops using integrability-based methods.

The connection with the DGLAP anomalous dimension, outlined above, is very important for the phenomenological strategy of the usage of the LL($\ln(1/z)$) resummation. Most of the common PDF sets⁴ use the fixed-order approximation for the DGLAP splittings/anomalous dimensions, i.e. no $\ln(1/z)$ -resummation is performed in the evolution. In particular, it means that existing LO, NLO and NNLO PDFs contain information only about the γ_N term in the series (2.20). Including further terms of this series into the CF coefficient function via the resummation will only increase the mismatch between the μ_F dependence of PDFs and the resummation factors and, hence, blow up our μ_F -scale uncertainty at high energy.

The goal of the present paper is to use HEF to cure the unphysical behaviour of the CF coefficient function at small z in a way consistent with the NLO DGLAP evolution of PDFs. Therefore, we will use the following *Doubly-Logarithmic approximation (DLA)* for resummation factor, which is obtained by neglecting all terms of the series (2.20) except the first one:

$$\mathcal{C}_{gg}^{\text{DLA}}(N, \mathbf{q}_T, \mu_F, \mu_R) = \frac{\gamma_N}{\mathbf{q}_T^2} \left(\frac{\mathbf{q}_T^2}{\mu_F^2} \right)^{\gamma_N}. \quad (2.28)$$

In the DLA, only terms $\propto \left(\frac{\alpha_s}{N} \ln \frac{\mathbf{q}_T^2}{\mu_F^2} \right)^n \leftrightarrow \alpha_s^n \ln^{n-1} \frac{1}{z} \ln^n \frac{\mathbf{q}_T^2}{\mu_F^2}$ are included in the resummation factor. One also takes $R(\gamma) = 1$ in the eqn. (2.28) for the same reason: the corresponding scheme-dependence starts at N³LO, eqn. (2.21), and is not taken into account in the NLO or even NNLO PDFs. The inclusion of this factor to the resummation function \mathcal{C} would only lead to an unphysical subtraction-scheme mismatch between the PDFs and the CF coefficient function.

The inverse Mellin transform:

$$\mathcal{C}(z, \mathbf{q}_T^2, \mu_F, \mu_R) = \int_{-i\infty}^{+i\infty} \frac{dN}{2\pi i} z^{-N} \mathcal{C}(N, \mathbf{q}_T^2, \mu_F, \mu_R), \quad (2.29)$$

of the resummation factor in the DLA can be computed straightforwardly, e.g. order-by-order in α_s with the use of relation (2.17), leading to the following result:

$$\mathcal{C}_{gg}^{\text{DLA}}(z, \mathbf{q}_T^2, \mu_F, \mu_R) = \frac{\hat{\alpha}_s(\mu_R)}{\mathbf{q}_T^2} \begin{cases} J_0 \left(2\sqrt{\hat{\alpha}_s(\mu_R) \ln\left(\frac{1}{z}\right) \ln\left(\frac{\mu_F^2}{\mathbf{q}_T^2}\right)} \right) & \text{if } \mathbf{q}_T^2 < \mu_F^2, \\ I_0 \left(2\sqrt{\hat{\alpha}_s(\mu_R) \ln\left(\frac{1}{z}\right) \ln\left(\frac{\mathbf{q}_T^2}{\mu_F^2}\right)} \right) & \text{if } \mathbf{q}_T^2 > \mu_F^2, \end{cases} \quad (2.30)$$

⁴With the notable exception of the sets obtained in refs. [50, 51].

where J_0/I_0 are Bessel functions of first/second kind. Eqn. (2.30) is known in the HEF community⁵ as the *(Collins-Ellis-)Blümlein formula*, and first appears in ref. [70] where the solution of the evolution equation written in ref. [44] has been studied.

The DLA resummation function (2.28), or equivalently (2.30), has a very important normalisation property:

$$\int_0^{\mu_F^2} d\mathbf{q}_T^2 \mathcal{C}_{gg}^{\text{DLA}}(N, \mathbf{q}_T^2, \mu_F, \mu_R) = 1 \leftrightarrow \int_0^{\mu_F^2} d\mathbf{q}_T^2 \mathcal{C}_{gg}^{\text{DLA}}(z, \mathbf{q}_T^2, \mu_F, \mu_R) = \delta(1-z), \quad (2.31)$$

which will be used extensively in the rest of the paper. The similar normalisation condition for \mathcal{C}_{gq} in the DLA follows from eqn. (2.22):

$$\int_0^{\mu_F^2} d\mathbf{q}_T^2 \mathcal{C}_{gq}^{\text{DLA}}(z, \mathbf{q}_T^2, \mu_F, \mu_R) = 0. \quad (2.32)$$

2.4 Small- z hard-scattering coefficient at NLO and NNLO from resummation

As a consistency check, the LL($\ln(1/z)$) resummation described above should reproduce the small- z behaviour (1.3) of the known NLO result for the coefficient function [28–30]. To this end, one has to expand the resummed CF coefficient functions (2.6) at least up to NLO in α_s . In this section, we perform such an expansion up to NNLO in order to provide predictions for the $\alpha_s^2 \ln(1/z)$ NNLO terms in the CF coefficient functions. The results of this section will also be employed in sec. 3.2 to construct the weight functions needed for our matching procedure. The DLA resummation factor (2.28) is appropriate for the expansion up to NNLO because the exact LL($\ln(1/z)$)-resummation factor (2.18) differs from it only starting at $\mathcal{O}(\alpha_s^3)$.

To perform such an expansion, it is convenient to work in Mellin space, plugging in the inverse Mellin transform (2.29) of eqns. (2.28) into eqn. (2.6). Passing to the dimensionless transverse momenta $\mathbf{n}_{T1} = \mathbf{q}_{T1}/M$ and $\mathbf{n}_{T2} = \mathbf{q}_{T2}/M$, one can rewrite the resummed CF coefficient functions as:

$$\hat{\sigma}_{ij}^{[m], \text{HEF}} = \sigma_0^{[m]} \int_{-\infty}^{\infty} d\eta \int_{-i\infty}^{+i\infty} \frac{dN_+ dN_-}{(2\pi i)^2} z^{-\frac{N_+ + N_-}{2}} e^{\eta(N_+ - N_-)} G_{ij}^{[m]} \left(\gamma_{N_+}, \gamma_{N_-}, \frac{N_+ + N_-}{2}, \frac{M^2}{\mu_F^2} \right), \quad (2.33)$$

where

$$G_{gg}^{[m]} \left(\gamma_1, \gamma_2, \nu, \frac{M^2}{\mu_F^2} \right) = \left(\frac{M^2}{\mu_F^2} \right)^{\gamma_1 + \gamma_2} \int_0^{\infty} \frac{\gamma_1 \gamma_2 d\mathbf{n}_{T1}^2 d\mathbf{n}_{T2}^2}{(\mathbf{n}_{T1}^2)^{1-\gamma_1} (\mathbf{n}_{T2}^2)^{1-\gamma_2}} \int_0^{2\pi} \frac{d\phi}{2\pi} f^{[m]}(\mathbf{n}_{T1}^2, \mathbf{n}_{T2}^2, \phi, \nu), \quad (2.34)$$

⁵See e.g. Ref. [69] for its application to the inclusive jet production at the LHC.

for the gluon channel, while for quark-induced channels, one takes into account eqn. (2.22) to obtain

$$G_{qg}^{[m]} = \left(\frac{M^2}{\mu_F^2}\right)^{\gamma_2} \frac{C_F}{C_A} \int_0^\infty \frac{\gamma_2 d\mathbf{n}_{T2}^2}{(\mathbf{n}_{T2}^2)^{1-\gamma_2}} \int_0^\infty d\mathbf{n}_{T1}^2 \left[\left(\frac{M^2}{\mu_F^2}\right)^{\gamma_1} \gamma_1 (\mathbf{n}_{T1}^2)^{-1+\gamma_1} - \delta(\mathbf{n}_{T1}^2) \right] \\ \times \int_0^{2\pi} \frac{d\phi}{2\pi} f^{[m]}(\mathbf{n}_{T1}^2, \mathbf{n}_{T2}^2, \phi), \quad (2.35)$$

and

$$G_{q\bar{q}}^{[m]} = \left(\frac{C_F}{C_A}\right)^2 \int_0^\infty d\mathbf{n}_{T1}^2 d\mathbf{n}_{T2}^2 \left[\left(\frac{M^2}{\mu_F^2}\right)^{\gamma_1} \gamma_1 (\mathbf{n}_{T1}^2)^{-1+\gamma_1} - \delta(\mathbf{n}_{T1}^2) \right] \\ \times \left[\left(\frac{M^2}{\mu_F^2}\right)^{\gamma_2} \gamma_2 (\mathbf{n}_{T2}^2)^{-1+\gamma_2} - \delta(\mathbf{n}_{T2}^2) \right] \int_0^{2\pi} \frac{d\phi}{2\pi} f^{[m]}(\mathbf{n}_{T1}^2, \mathbf{n}_{T2}^2, \phi), \quad (2.36)$$

where, in eqns. (2.34), (2.35) and (2.36), the dimensionless function

$$f^{[m]}(\mathbf{n}_{T1}^2, \mathbf{n}_{T2}^2, \phi, \nu) = \frac{\pi H^{[m]}(M^2 \mathbf{n}_{T1}^2, M^2 \mathbf{n}_{T2}^2, \phi)}{\sigma_0^{[m]} M^4 (1 + (\mathbf{n}_{T1} + \mathbf{n}_{T2})^2)^{2+\nu}} = \frac{F^{[m]}(M^2 \mathbf{n}_{T1}^2, M^2 \mathbf{n}_{T2}^2, \phi)}{(1 + (\mathbf{n}_{T1} + \mathbf{n}_{T2})^2)^{2+\nu}}, \quad (2.37)$$

encapsulates the HEF coefficient function $H^{[m]}$ (or $F^{[m]}$ of eqn. (2.11)) and the kinematic factor $1/M_T^4$ from eqn. (2.6).

The only quantity depending on α_s in eqn. (2.33) is $\gamma_N = \hat{\alpha}_s/N$. One thus only has to Taylor-expand the function $G_{ij}^{[m]}$ with respect to its arguments γ_{N_+} and γ_{N_-} . The corresponding poles in N_+ and N_- map to the following functions of z via eqn. (2.33):

$$1 \rightarrow \delta(1-z), \\ \frac{1}{N_+} \text{ and } \frac{1}{N_-} \rightarrow \theta(1-z), \\ \frac{1}{N_+^2}, \frac{1}{N_-^2}, \text{ and } \frac{1}{N_+ N_-} \rightarrow \theta(1-z) \ln \frac{1}{z}. \quad (2.38)$$

The expansion of the $\mathbf{n}_{T1,2}^2$ integrand of the function $G_{ij}^{[m]}$ in γ_1 and γ_2 however has to be done in a distributional sense because otherwise the order-by-order integrals will just diverge at $\mathbf{n}_{T1,2}^2 \rightarrow 0$. To this end, one isolates the $\mathbf{n}_{T1,2}^2 \rightarrow 0$ behaviour of the $f^{[m]}$ function⁶ in the integrands of eqns. (2.34), (2.35) and (2.36) as follows:

$$f^{[m]}(\mathbf{n}_{T1}^2, \mathbf{n}_{T2}^2, \phi, \nu) = \\ \left\{ f^{[m]}(\mathbf{n}_{T1}^2, \mathbf{n}_{T2}^2, \phi, \nu) - f^{[m]}(0, \mathbf{n}_{T2}^2, \phi, \nu) \theta(1 - \mathbf{n}_{T1}^2) \right. \\ \left. - f^{[m]}(\mathbf{n}_{T1}^2, 0, \phi, \nu) \theta(1 - \mathbf{n}_{T2}^2) + f^{[m]}(0, 0, \phi, \nu) \theta(1 - \mathbf{n}_{T1}^2) \theta(1 - \mathbf{n}_{T2}^2) \right\} \\ + \left[f^{[m]}(\mathbf{n}_{T1}^2, 0, \phi, \nu) - f^{[m]}(0, 0, \phi, \nu) \theta(1 - \mathbf{n}_{T1}^2) \right] \theta(1 - \mathbf{n}_{T2}^2) \\ + \left[f^{[m]}(0, \mathbf{n}_{T2}^2, \phi, \nu) - f^{[m]}(0, 0, \phi, \nu) \theta(1 - \mathbf{n}_{T2}^2) \right] \theta(1 - \mathbf{n}_{T1}^2) \\ + f^{[m]}(0, 0, \phi, \nu) \theta(1 - \mathbf{n}_{T1}^2) \theta(1 - \mathbf{n}_{T2}^2). \quad (2.39)$$

⁶Which can be understood as a test function, on which functionals (2.34), (2.35) and (2.36) depend.

The expression in curly brackets in eqn. (2.39) tends to zero when $\mathbf{n}_{T1}^2 \rightarrow 0$ and/or $\mathbf{n}_{T2}^2 \rightarrow 0$, so the factors $(\mathbf{n}_{T1}^2)^{-1+\gamma_1}$ and $(\mathbf{n}_{T2}^2)^{-1+\gamma_2}$ in front of it in eqns. (2.34) – (2.36) can be safely Taylor-expanded in $\gamma_{1,2}$. The expression in the fourth line of eqn. (2.39) tends to zero when $\mathbf{n}_{T1}^2 \rightarrow 0$ while its dependence on \mathbf{n}_{T2}^2 is just a step function. As a consequence, when this expression is substituted to eqns. (2.34) – (2.36), the dependence on \mathbf{n}_{T2}^2 can be integrated out, while the factor $(\mathbf{n}_{T1}^2)^{-1+\gamma_1}$ can be Taylor-expanded in γ_1 . For the term in the fifth line of eqn. (2.39), the situation is symmetric, up to the replacement $\mathbf{n}_{T1} \leftrightarrow \mathbf{n}_{T2}$. Finally, with the last term in eqn. (2.39), the integrations over \mathbf{n}_{T1}^2 and \mathbf{n}_{T2}^2 can be performed straightforwardly. The resulting expansions for the functions $G_{ij}^{[m]}$ in γ_1 and γ_2 at $\nu = 0$ are:

$$G_{gg}^{[m]} = \left(\frac{M^2}{\mu_F^2}\right)^{\gamma_1+\gamma_2} \left[A_0^{[m]} + (\gamma_1 + \gamma_2)A_1^{[m]} + (\gamma_1^2 + \gamma_2^2)A_2^{[m]} + \gamma_1\gamma_2 B_2^{[m]} + \mathcal{O}(\gamma^3) \right]. \quad (2.40)$$

$$G_{qg}^{[m]} = \frac{C_F}{C_A} \left(\frac{M^2}{\mu_F^2}\right)^{\gamma_2} \left\{ \left[\left(\frac{M^2}{\mu_F^2}\right)^{\gamma_1} - 1 \right] A_0^{[m]} + \left(\frac{M^2}{\mu_F^2}\right)^{\gamma_1} (\gamma_1 A_1^{[m]} + \gamma_1^2 A_2^{[m]}) \right. \\ \left. + \left[\left(\frac{M^2}{\mu_F^2}\right)^{\gamma_1} - 1 \right] (\gamma_2 A_1^{[m]} + \gamma_2^2 A_2^{[m]}) + \left(\frac{M^2}{\mu_F^2}\right)^{\gamma_1} \gamma_1 \gamma_2 B_2^{[m]} + \mathcal{O}(\gamma^3) \right\}, \quad (2.41)$$

$$G_{q\bar{q}}^{[m]} = \left(\frac{C_F}{C_A}\right)^2 \left\{ \left[\left(\frac{M^2}{\mu_F^2}\right)^{\gamma_1} - 1 \right] \left[\left(\frac{M^2}{\mu_F^2}\right)^{\gamma_2} - 1 \right] A_0^{[m]} \right. \\ \left. + \left[\left(\frac{M^2}{\mu_F^2}\right)^{\gamma_2} - 1 \right] \left(\frac{M^2}{\mu_F^2}\right)^{\gamma_1} (\gamma_1 A_1^{[m]} + \gamma_1^2 A_2^{[m]}) \right. \\ \left. + \left[\left(\frac{M^2}{\mu_F^2}\right)^{\gamma_1} - 1 \right] \left(\frac{M^2}{\mu_F^2}\right)^{\gamma_2} (\gamma_2 A_1^{[m]} + \gamma_2^2 A_2^{[m]}) + \left(\frac{M^2}{\mu_F^2}\right)^{\gamma_1+\gamma_2} \gamma_1 \gamma_2 B_2^{[m]} + \mathcal{O}(\gamma^3) \right\}, \quad (2.42)$$

where the Taylor expansion of the factors $(M^2/\mu_F^2)^{\gamma_{1,2}}$ up to the second order have to be done as well. The coefficients $A_{0,1,2}^{[m]}$ entering this expansion are:

$$A_0^{[m]} = \int_0^{2\pi} \frac{d\phi}{2\pi} f^{[m]}(0, 0, \phi, 0), \quad (2.43)$$

$$A_1^{[m]} = \int_0^\infty \frac{d\mathbf{n}_{T1}^2}{\mathbf{n}_{T1}^2} \int_0^{2\pi} \frac{d\phi}{2\pi} \left[f^{[m]}(\mathbf{n}_{T1}^2, 0, \phi, 0) - f^{[m]}(0, 0, \phi, 0)\theta(1 - \mathbf{n}_{T1}^2) \right], \quad (2.44)$$

$$A_2^{[m]} = \int_0^\infty \frac{d\mathbf{n}_{T1}^2}{\mathbf{n}_{T1}^2} \ln \mathbf{n}_{T1}^2 \int_0^{2\pi} \frac{d\phi}{2\pi} \left[f^{[m]}(\mathbf{n}_{T1}^2, 0, \phi, 0) - f^{[m]}(0, 0, \phi, 0)\theta(1 - \mathbf{n}_{T1}^2) \right], \quad (2.45)$$

while, for the coefficient $B_2^{[m]}$, one has

$$B_2^{[m]} = \int_0^\infty \frac{d\mathbf{n}_{T1}^2 d\mathbf{n}_{T2}^2}{\mathbf{n}_{T1}^2 \mathbf{n}_{T2}^2} \int_0^{2\pi} \frac{d\phi}{2\pi} \left\{ f^{[m]}(\mathbf{n}_{T1}^2, \mathbf{n}_{T2}^2, \phi, 0) - f^{[m]}(0, \mathbf{n}_{T2}^2, \phi, 0)\theta(1 - \mathbf{n}_{T1}^2) \right. \\ \left. - f^{[m]}(\mathbf{n}_{T1}^2, 0, \phi, 0)\theta(1 - \mathbf{n}_{T2}^2) + f^{[m]}(0, 0, \phi, 0)\theta(1 - \mathbf{n}_{T1}^2)\theta(1 - \mathbf{n}_{T2}^2) \right\}. \quad (2.46)$$

State	$A_0^{[m]}$	$A_1^{[m]}$	$A_2^{[m]}$	$B_2^{[m]}$
1S_0	1	-1	$\frac{\pi^2}{6}$	$\frac{\pi^2}{6}$
3S_1	0	1	0	$\frac{\pi^2}{6}$
3P_0	1	$-\frac{43}{27}$	$\frac{\pi^2}{6} + \frac{2}{3}$	$\frac{\pi^2}{6} + \frac{40}{27}$
3P_1	0	$\frac{5}{54}$	$-\frac{1}{9}$	$-\frac{2}{9}$
3P_2	1	$-\frac{53}{36}$	$\frac{\pi^2}{6} + \frac{1}{2}$	$\frac{\pi^2}{6} + \frac{11}{9}$

Table 1. Coefficients entering into eqns. (2.47) – (2.49) for several states $m = {}^{2S+1}L_J$ of a $Q\bar{Q}$ pair. The highlighted numbers coincide with the corresponding results from the table 1 in ref. [30].

Substituting the expansion (2.40) to eqn. (2.33) due to the mappings (2.38), one obtains the following result for the z -dependent CF coefficient function in gg channel:

$$\hat{\sigma}_{gg}^{[m], \text{HEF}} = \sigma_0^{[m]} \left\{ A_0^{[m]} \delta(1-z) + \frac{\alpha_s}{\pi} 2C_A \left[A_1^{[m]} + A_0^{[m]} \ln \frac{M^2}{\mu_F^2} \right] \right. \\ \left. + \left(\frac{\alpha_s}{\pi} \right)^2 C_A^2 \ln \frac{1}{z} \left[2A_2^{[m]} + B_2^{[m]} + 4A_1^{[m]} \ln \frac{M^2}{\mu_F^2} + 2A_0^{[m]} \ln^2 \frac{M^2}{\mu_F^2} \right] + \mathcal{O}(\alpha_s^3) \right\}, \quad (2.47)$$

where $\sigma_0^{[m]}$ has been defined in eqn. (2.12). The coefficients $A_{0,1,2}^{[m]}$ and $B_2^{[m]}$ can be computed for various spin-orbital states $m = {}^{2S+1}L_J$ by substituting the HEF coefficient functions from eqn. (2.15) to eqns. (2.43), (2.44), (2.45) and (2.46). The results of this computation are listed in the table 1.

Similarly, from the expansions (2.41) and (2.42), one obtains the following predictions for the small- z behaviour of the quark-induced channels at NLO and NNLO:

$$\hat{\sigma}_{qg}^{[m], \text{HEF}} = \sigma_0^{[m]} \left\{ \frac{\alpha_s}{\pi} C_F \left[A_1^{[m]} + A_0^{[m]} \ln \frac{M^2}{\mu_F^2} \right] + \left(\frac{\alpha_s}{\pi} \right)^2 C_A C_F \ln \frac{1}{z} \right. \\ \left. \times \left[A_2^{[m]} + B_2^{[m]} + 3A_1^{[m]} \ln \frac{M^2}{\mu_F^2} + \frac{3}{2} A_0^{[m]} \ln^2 \frac{M^2}{\mu_F^2} \right] \right\}, \quad (2.48)$$

$$\hat{\sigma}_{q\bar{q}}^{[m], \text{HEF}} = \sigma_0^{[m]} \left(\frac{\alpha_s}{\pi} \right)^2 C_F^2 \ln \frac{1}{z} \left[B_2^{[m]} + 2A_1^{[m]} \ln \frac{M^2}{\mu_F^2} + A_0^{[m]} \ln^2 \frac{M^2}{\mu_F^2} \right]. \quad (2.49)$$

Where the same coefficients $A_{0,1,2}^{[m]}$ and $B_2^{[m]}$ appear as in the gg case. The NLO parts of eqns. (2.47) and (2.48) coincide with the $z \rightarrow 0$ asymptotics of the full NLO results, obtained in refs. [30, 32], which is yet another non-trivial cross-check of the HEF formalism.

Let us emphasise that the specific transverse-momentum dependence of the HEF coefficient functions is crucial for the consistency of the HEF results with the high-energy limit of the QCD scattering amplitudes. This is very different from the case of TMD factorisation, which is applicable only at $\mathbf{p}_T^2 \ll M^2$. The NLO coefficient $A_1^{[m]}$ is determined by the behaviour of the coefficient function for $\mathbf{p}_T^2 \simeq \mathbf{q}_{T1,2}^2 \sim M^2$ as follows. In the integrand of eqn. (2.44), the step-function $\theta(1 - \mathbf{n}_{T1}^2)$ is subtracted from the dimensionless

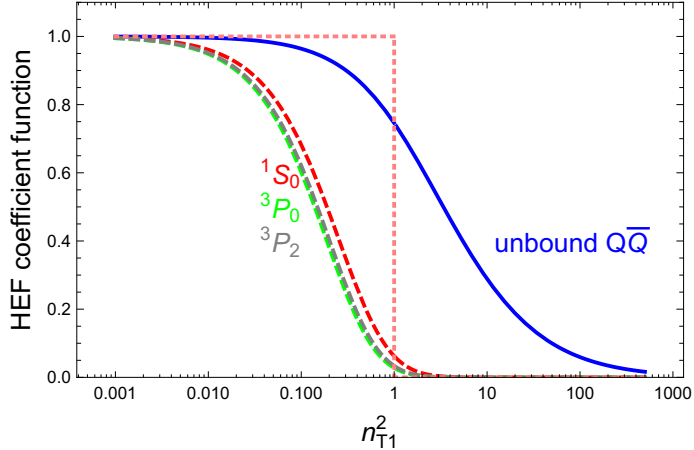


Figure 2. Dimensionless integrand function (2.37) averaged over ϕ , at $\mathbf{n}_{T_2}^2 = 0$, as a function of $\mathbf{n}_{T_1}^2 = \mathbf{q}_{T_1}^2/(4m_Q^2)$, normalised on its value at $\mathbf{n}_{T_1}^2 = 0$. The three dashed curves correspond to the coefficient functions for production of $Q\bar{Q}[m]$ -states with $m = {}^1S_0, {}^3P_0$ and 3P_2 (section 2.2). The solid curve depicts the coefficient function for the unbound $Q\bar{Q}$ -pair production [37], integrated over the phase space of the $Q\bar{Q}$ pair. The short-dashed line represents the $\overline{\text{MS}}$ subtraction term $\theta(1 - \mathbf{n}_{T_1}^2)$.

function $f^{[m]}(\mathbf{n}_{T_1}^2, 0, \phi, 0)$, which describes the coefficient function in the case when one gluon is off-shell with momenta $\mathbf{q}_{T,1}$ and the second one is on-shell $\mathbf{q}_{T,2}^2 = 0$. In the case of quarkonia, the latter function starts to decrease already for $\mathbf{n}_{T_1}^2 = \mathbf{q}_{T_1}^2/M^2 < 1$, so the subtraction leads to a large negative contribution, as illustrated by the plot in the figure 2. For comparison, the coefficient function for open heavy flavour production, integrated over the phase-space of the final-state heavy quarks, given by eqns. (4.8) – (4.10) in ref. [37], is also plotted in figure 2. From this figure, one immediately realises that the bound state is easily broken by the transverse-momentum imbalance between the incoming off-shell gluons, which leads to a quickly decreasing HEF coefficient function. This dependence is quite different from the “expectation” of the $\overline{\text{MS}}$ scheme⁷, according to which the coefficient function should behave roughly like $\theta(1 - \mathbf{q}_{T_{1,2}}^2/M^2)$ thus leading to the consequent over-subtraction of the collinear behaviour. For the case of open heavy flavour, integrated over its invariant mass, the situation is opposite and the coefficient function has a substantial tail at $\mathbf{q}_{T_{1,2}}^2 > M^2$, which leads to large positive NLO corrections at high energy.

2.5 Resummation by a μ_F choice

The connection between the HEF resummation and the μ_F -scale optimisation approach (the $\hat{\mu}_F$ prescription) proposed in ref. [30] is most easily illustrated by eqn. (2.34). Substi-

⁷See e.g. section 3.4 of ref. [56] for the relation of the $\overline{\text{MS}}$ subtraction of $1/\epsilon$ singularity with the transverse momentum cut off.

tuting the scale choice (1.4), one obtains:

$$G_{gg}^{[m]} \left(\gamma_{N_+}, \gamma_{N_-}, \nu, \frac{M^2}{\hat{\mu}_F^2} \right) = \exp \left[-A_1^{[m]} (\gamma_{N_+} + \gamma_{N_-}) \right] \quad (2.50)$$

$$\times \int_0^\infty \frac{\gamma_{N_+} \gamma_{N_-} d\mathbf{n}_{T1}^2 d\mathbf{n}_{T2}^2}{(\mathbf{n}_{T1}^2)^{1-\gamma_{N_+}} (\mathbf{n}_{T2}^2)^{1-\gamma_{N_-}}} \int_0^{2\pi} \frac{d\phi}{2\pi} f^{[m]}(\mathbf{n}_{T1}^2, \mathbf{n}_{T2}^2, \phi, \nu).$$

The exponent in the first line of eqn. (2.50), which arose from the scale choice (1.4), resums a series of corrections proportional to $\gamma_{N_\pm}^n = \hat{\alpha}_s^n / N_\pm^n$, which belong to the LL($\ln(1/z)$)-approximation. This resummation would be equivalent to that performed by the HEF only if this exponent is able to cancel the γ_{N_\pm} dependence of the integral in the second line of eqn. (2.50). If this was the case then all LL($\ln(1/z)$) corrections would be removed from the CF coefficient function and absorbed into the scale evolution of PDFs. However, such a perfect cancellation is possible only if the dimensionless function $f^{[m]}$ complies to the relation:

$$\int_0^{2\pi} \frac{d\phi}{2\pi} f^{[m]}(\mathbf{n}_{T1}^2, \mathbf{n}_{T2}^2, \phi, \nu) = \theta \left(e^{A_1^{[m]}} - \mathbf{n}_{T1}^2 \right) \theta \left(e^{A_1^{[m]}} - \mathbf{n}_{T2}^2 \right), \quad (2.51)$$

which when substituted to the eqn. (2.50) leads to $G_{gg}^{[m]}(\gamma_{N_+}, \gamma_{N_-}, \nu, M^2/\hat{\mu}_F^2) = 1$. Neither the coefficient functions for quarkonium production listed in the section 2.2, nor any other coefficient functions for physical processes known to the authors provide a sharp cut-off in the transverse momentum as in eqn. (2.51). Instead, they always smoothly depend on transverse momenta, as e.g. in the figure 2. Therefore, the HEF is not equivalent to the $\hat{\mu}_F$ prescription. By construction, the $\hat{\mu}_F$ prescription takes into account the coefficient $A_1^{[m]}$ and, hence, it is correct up to NLO in α_s . However, already at NNLO in α_s , the results of HEF and the $\hat{\mu}_F$ prescription differ. This is clear because the NNLO coefficients obtained from HEF (table 1) contain the transcendental number $\pi^2/6$, which can not arise from the expansion of the exponent in the first line of eqn. (2.50).

3 NLO+DLA matching in z -space

Before discussing various approaches to match the DLA HEF and NLO CF contributions into a single prediction for the total cross section, let us set the baseline by showing how the NLO CF cross section with the “canonical” scale choice $\mu_F = \mu_R = M$ depends on the energy and how large the associated scale uncertainty is. The plots of figure 3 show the LO and NLO CF predictions for the total cross section of the production of $^1S_0^{[1]}$ states with masses of 3 and 9.4 GeV. The scale uncertainties, depicted as solid or shaded bands in all these plots, has been estimated using the five-point scale-variation procedure. The latter procedure consists in evaluating the cross section for each value of the energy with the scale choice $\mu_F = 2^{\zeta_1} M$ and $\mu_R = 2^{\zeta_2} M$ for $(\zeta_1, \zeta_2) \in \{(0, \pm 1), (\pm 1, 0)\}$ and taking, as an uncertainty estimate, the largest positive or negative deviation of the obtained value from the cross section with the default scale choice.

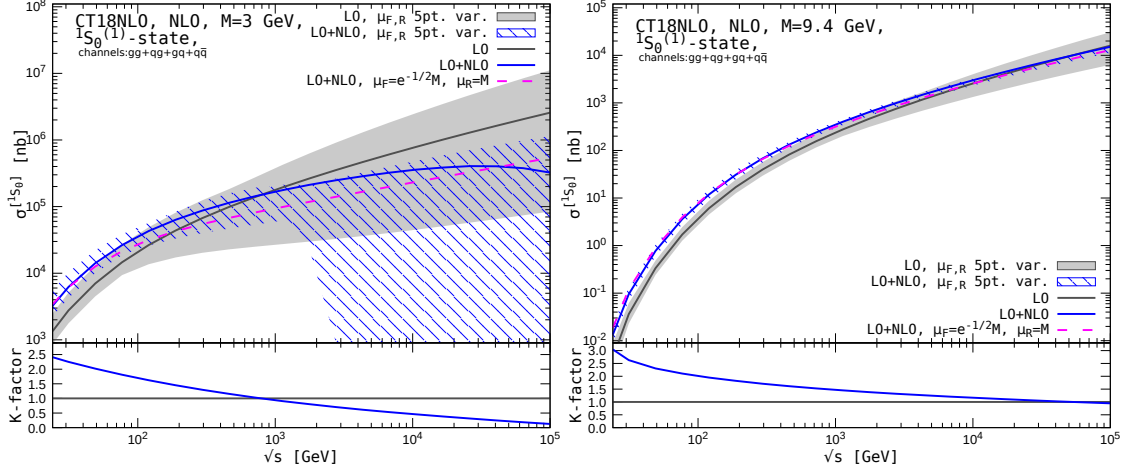


Figure 3. Comparison of the energy dependence of the hadroproduction cross sections of a $Q\bar{Q}[^1S_0^{(1)}]$ state with $M = 3$ GeV (**left panel**) and $M = 9.4$ GeV (**right panel**) in CF at LO (grey curve) and NLO (blue curve). The central member of the CT18NLO PDF set [71] has been used. The dashed line depicts the central prediction of the NLO calculation using the $\hat{\mu}_F$ prescription (Equation 1.4) [30]. The LDME $\langle\mathcal{O}[^1S_0^{(1)}]\rangle$ was set to 1 GeV^3 in both cases for illustration purposes.

From the left panel of figure 3, one can see that, for $c\bar{c}$ states, the instability of the cross section at high energy is dramatic. Above $\sqrt{s} = 1 \text{ TeV}$, such a computation does not show any more predictive power and, above $\sqrt{s} = 100 \text{ GeV}$, the NLO K factor, defined as the ratio of the NLO to the LO cross section, decreases with energy, which is very different from the behaviour of the matched result as we will see. For bottomonia (see the plot in the right panel of figure 3), the situation is much better: the scale uncertainty of the NLO calculation is significantly smaller than the LO one all the way up to $\sqrt{s} \sim 100 \text{ TeV}$. However, the decrease of the NLO K factor is evident even at this scales. The dependence of this behaviour on the PDF choice has been analysed in detail in ref. [30].

A specific factorisation scale choice (1.4) has been proposed in ref. [30] as a possible resolution of the problem of high-energy instability of quarkonium hadroproduction cross sections. As we have shown in section 2.5, this prescription is equivalent to the resummation of some $\text{LL}(\ln 1/z)$ -terms, which is correct at NLO but fails at higher orders. In practice, this procedure leads to significantly smaller cross section at high energies, shown by dashed lines in figure 3, than that predicted by LO CF at the default scale.

The DL HEF resummation proposed in section 2.3 is compatible with the factorisation scheme and the evolution of the usual NLO and NNLO PDFs and correctly reproduces the $\text{LL}(\ln 1/z)$ terms in the CF coefficient function up to NNLO in α_s , as it was shown in sections 2.3 and 2.4. However this resummation is applicable only in the region of $z \ll 1$. Power corrections $\mathcal{O}(z)$ to the CF coefficient function are missing in the HEF calculation with any $N^k\text{LL}$ accuracy, while they are equally important as the logarithmic terms at $z \sim 1$. For the value of the total cross section, the whole range of z from 0 to 1 contributes due to the integration over z in eqn. (1.1). In the following subsections, we will propose

two approaches to match these DL HEF and NLO CF results in z space and will compare the corresponding numerical results.

3.1 The subtractive-matching prescription

The simplest matching prescription between NLO CF and DLA HEF calculations consists in the subtraction of the $z \rightarrow 0$ asymptotics of the NLO CF coefficient function, to avoid double-counting it with the HEF contribution:

$$\sigma_{\text{NLO+HEF}}^{[m]} = \sigma_{\text{LO CF}}^{[m]} + \sum_{i,j=q,\bar{q},g,z_{\min}} \int \frac{dz}{z} \left[\check{\sigma}_{\text{HEF}}^{[m],ij}(z) + \hat{\sigma}_{\text{NLO CF}}^{[m],ij}(z) - \hat{\sigma}_{\text{NLO CF}}^{[m],ij}(0) \right] \mathcal{L}_{ij}(z), \quad (3.1)$$

where $\check{\sigma}_{\text{HEF}}^{[m],gg}$ is defined in eqn. (2.7) while, for other partonic channels, $\check{\sigma}_{\text{HEF}}^{[m],ij} = \hat{\sigma}_{\text{HEF}}^{[m],ij}$ and $\hat{\sigma}_{\text{NLO CF}}^{[m],ij}(z)$ includes only the $\mathcal{O}(\alpha_s)$ CF terms from the original papers [28, 29].

The corresponding numerical results for $Q\bar{Q}[^1S_0^{(1)}]$ states with masses of 3 and 9.4 GeV are shown in the figure 4. One can see that the high-energy instability of the NLO cross section has gone away and the ratio of the matched cross section to the LO one becomes almost constant at high energy, which signal that energy dependence is now mostly driven by the PDFs, not by the hard-scattering coefficient.

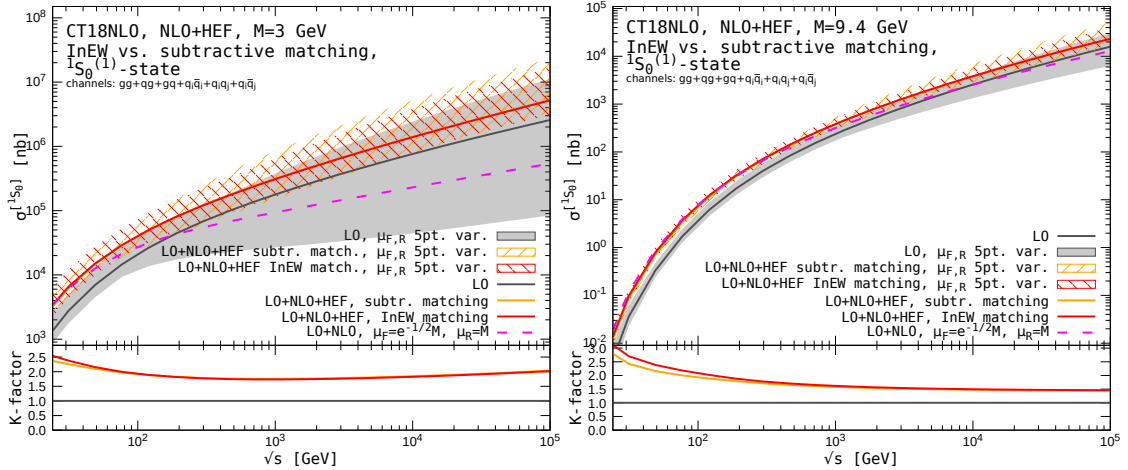


Figure 4. Comparison of the energy dependence of the hadroproduction cross sections of a $Q\bar{Q}[^1S_0^{(1)}]$ state with $M = 3$ GeV (**left panel**) and $M = 9.4$ GeV (**right panel**) for the matched NLO CF + DLA HEF calculations using the subtractive (orange curve and right-shaded band) and InEW matchings with $\kappa_{\text{CF}} = 0$ and $\kappa_{\text{HEF}} = 0$ (red curve and left-shaded band). The dashed line depicts the central prediction of the NLO calculation using the $\hat{\mu}_F$ prescription (Equation 1.4) [30]. The LDME $\langle \mathcal{O}[^1S_0^{(1)}] \rangle$ was set to 1 GeV^3 .

3.2 The inverse-error-weighting matching

The InEW matching method has been proposed in ref. [52] to match the $|\mathbf{p}_{Tl+l-}|$ spectrum of Drell-Yan lepton pairs predicted by the TMD factorisation for $|\mathbf{p}_{Tl+l-}| \ll M_{l+l-}$ with

the NLO CF calculation of the same spectrum, which is free from large logarithms of $|\mathbf{p}_{Tl+l-}|/M_{l+l-}$ for $|\mathbf{p}_{Tl+l-}| \gtrsim M_{l+l-}$. Following the same ideas, we introduce smooth weight functions $w_{\text{HEF}}(z)$ and $w_{\text{CF}}(z)$ into our cross section formula as follows:

$$\begin{aligned} \sigma_{\text{NLO+HEF}}^{[m]} &= \sigma_{\text{LO CF}}^{[m]} + \\ &+ \sum_{i,j=q,\bar{q},g,z_{\min}} \int_0^1 dz \left\{ \left[\hat{\sigma}_{\text{HEF}}^{[m],ij}(z) \frac{\mathcal{L}_{ij}(z)}{z} \right] w_{\text{HEF}}^{ij}(z) + \left[\hat{\sigma}_{\text{NLO CF}}^{[m],ij}(z) \frac{\mathcal{L}_{ij}(z)}{z} \right] w_{\text{CF}}^{ij}(z) \right\}, \end{aligned} \quad (3.2)$$

where we emphasise that the weights are introduced on the level of the z integrand of the cross section, so that the distributions $1/(1-z)_+$ and $\ln(1-z)/(1-z)_+$, contained in the $\hat{\sigma}_{\text{NLO CF},ij}^{[m]}$, have already ‘‘acted’’ on the function $\mathcal{L}_{ij}(z)/z$. The weights should suppress one of the contributions in the region where it is unreliable, so naturally they are chosen to be proportional to the inverse squared errors of each contribution and to add up to one:

$$w_{\text{HEF}}^{ij}(z) = \frac{[\Delta\sigma_{\text{HEF}}^{ij}(z)]^{-2}}{[\Delta\sigma_{\text{HEF}}^{ij}(z)]^{-2} + [\Delta\sigma_{\text{CF}}^{ij}(z)]^{-2}}, \quad w_{\text{CF}}^{ij}(z) = 1 - w_{\text{HEF}}^{ij}(z), \quad (3.3)$$

where, by $\Delta\sigma_{\text{HEF}/\text{CF}}^{ij}$, we refer to an estimate of the theoretical uncertainty of the corresponding contributions to the z integrand of the total cross section, which should correctly capture the fact that the HEF or the CF contributions respectively become unreliable in the $z \rightarrow 1$ or $z \rightarrow 0$ limits. The integrand uncertainty due to the matching procedure then follows from:

$$\Delta\sigma_{\text{Match.}}^{ij}(z) = \left([\Delta\sigma_{\text{HEF}}^{ij}(z)]^{-2} + [\Delta\sigma_{\text{CF}}^{ij}(z)]^{-2} \right)^{-1/2}, \quad (3.4)$$

which, upon integration over z , gives the total cross-section uncertainty.

The errors entering eqns. (3.3) and (3.4) can be estimated as follows. The NLO CF cross section contains no information about the small- z behaviour of $\hat{\sigma}^{[m],ij}(z)$ beyond $\mathcal{O}(\alpha_s)$, while HEF provides this information. Hence one can take the $\mathcal{O}(\alpha_s^2)$ expansion of the HEF cross section, obtained in Sec. 2.4 as an estimate for the error of NLO CF integrand:

$$\Delta\sigma_{\text{CF}}^{ij}(z) = \sigma_{\text{LO}} \left(\frac{\alpha_s}{\pi} \right)^2 \left[C_{\text{LL}}^{ij} \ln \frac{1}{z} + (1-z)\kappa_{\text{CF}} \right] \frac{\mathcal{L}_{ij}(z)}{z}, \quad (3.5)$$

where

$$C_{\text{LL}}^{gg} = C_A^2 \left[2A_2 + B_2 + 4A_1 \ln \frac{M^2}{\mu_F^2} + 2A_0 \ln^2 \frac{M^2}{\mu_F^2} \right], \quad (3.6)$$

$$C_{\text{LL}}^{qg} = C_A C_F \left[A_2 + B_2 + 3A_1 \ln \frac{M^2}{\mu_F^2} + \frac{3}{2} A_0 \ln^2 \frac{M^2}{\mu_F^2} \right], \quad (3.7)$$

$$C_{\text{LL}}^{q\bar{q}} = C_F^2 \left[B_2 + 2A_1 \ln \frac{M^2}{\mu_F^2} + A_0 \ln^2 \frac{M^2}{\mu_F^2} \right], \quad (3.8)$$

and the coefficients $A_0, A_{1,2}, B_2$ can be found in table 1, while the coefficient κ_{CF} stands for the constant part of the $z \rightarrow 0$ behaviour of the NNLO partonic cross section, which is currently unknown because it belongs to the NLL approximation of HEF.

Conversely, the HEF coefficient function contains no information about the $\mathcal{O}(z)$ power corrections, while the LO CF coefficient function contains this corrections at NLO in α_s . Hence one can take the NLO CF hard-scattering coefficient with its $z \rightarrow 0$ asymptotics subtracted, as an estimate of the missing $\mathcal{O}(z)$ power corrections in HEF, i.e. of its error:

$$\Delta\sigma_{\text{HEF}}^{ij}(z) = \left[\hat{\sigma}_{\text{NLO CF}}^{[m],ij}(z) - \hat{\sigma}_{\text{NLO CF}}^{[m],ij}(0) + \sigma_{\text{LO}} \left(\frac{\alpha_s}{\pi} \right)^2 z \kappa_{\text{HEF}} \right] \frac{\mathcal{L}_{ij}(z)}{z}, \quad (3.9)$$

where the parameter κ_{HEF} stands for the unknown $z \rightarrow 1$ behaviour of the coefficient function in CF at NNLO in α_s .

Using formulas (3.5) and (3.9), one can construct weights w_{CF} and w_{HEF} with expected behaviour: e.g. $w_{\text{CF}}(z)$ goes to 1 when $z \rightarrow 1$ and to 0 when $z \rightarrow 0$ and conversely for w_{HEF} . The latter property is ensured by the behaviour of errors (3.5) and (3.9). The CF error (3.5) is 0 for $z = 1$ and increases towards $z \rightarrow 0$, while HEF error (3.9) is zero at $z = 0$, and increases towards $z = 1$.

In figures 5, 6 and 7 several plots of the z integrand of eqn. (3.2) are shown as red solid lines, using weights obtained above with $\kappa_{\text{HEF}} = 0$ and $\kappa_{\text{CF}} = 0$. One can see that the aforementioned procedure provides a smooth interpolation between the HEF curves at $z \ll 1$ and the CF curves at z closer to 1. Curiously, the matching of HEF and CF contributions happens approximately at the point of intersection of HEF and CF curves.

The corresponding curves for the subtractive matching are shown for comparison by the red dotted lines. From figures 5, 6 and 7, the problem of subtractive matching is evident: it subtracts the $z \rightarrow 0$ asymptotics of the NLO CF coefficient function at all values of z , thus introducing the unphysical modification of the $z \rightarrow 1$ behaviour. The InEW matching, on the other hand, smoothly connects the asymptotic regions.

The sensitivity of the weights on the parameters κ_{CF} and κ_{HEF} is shown in the Fig. 8. The curves corresponding to the maximal variation of weights for $\kappa_{\text{HEF}/\text{CPM}} = \pm 1$ are plotted as dashed lines. The variation of w_{CF}^{gg} is quite moderate, while larger variations of other weights are observed, they are not important for the value of the total cross section, because these contributions are small.

The results for the matched cross section in the InEW procedure with $\kappa_{\text{CF}} = 0$ and $\kappa_{\text{HEF}} = 0$ are shown by red solid curves on figure 4. The matching uncertainty, estimated by eqn. (3.4), combined with the uncertainty due to the variation of $\kappa_{\text{CPM}/\text{HEF}} \in [-1, 1]$ amounts to about 10% compared to the central LO cross section, so it is negligible in comparison with the scale uncertainties shown on figure 4. The scale uncertainty band is slightly smaller in the InEW matching case. Probably the better measure of the uncertainty due to the matching procedure is the difference between central results obtained in the subtractive and InEW matching approaches and it turns out to be non-negligible only for $\sqrt{s} < 100$ GeV.

Finally, figure 9 illustrates how the matched cross section varies depending on the choice of the collinear PDF. Since our computations are rather computer intensive, only the central members of the CT18NLO [71], MSHT20nlo_as118 [72], NNPDF31_nlo_as_0118 [73] and NNPDF31sx_nlon11x_as_0118 [50] PDF sets, as implemented in the LHAPDF library [74] has been used for the comparison. The first three PDFs evolve according to the usual

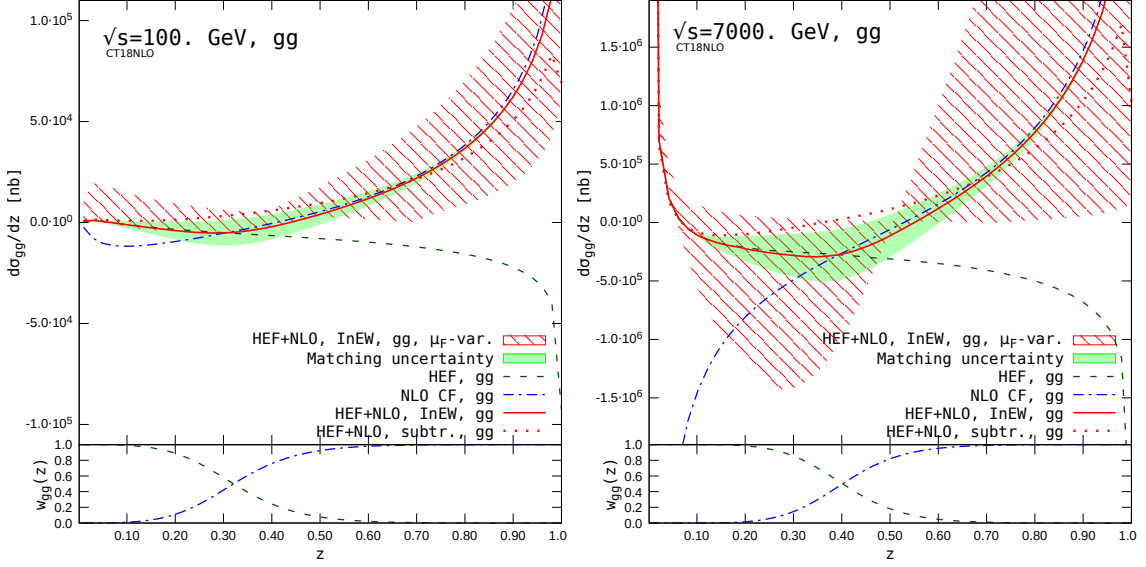


Figure 5. Matching plots for the gg -channel contribution to the $^1S_0^{[1]}$ -state hadroproduction with $M = 3$ GeV. The solid curve depicts the z -integrand of eqn. (3.2), the dashed curve the HEF contribution (without the InEW weight), the dash-dotted curve the NLO CF contribution (without the InEW weight), and the dotted red line the integrand of eqn. (3.1), i.e. the result of the subtractive matching prescription for comparison. The plots of the InEW weights are shown in the bottom inset, while the matching uncertainty (3.4) is shown as the solid band. The LDME $\langle \mathcal{O}[^1S_0^{[1]}] \rangle$ was set to 1 GeV^3 .

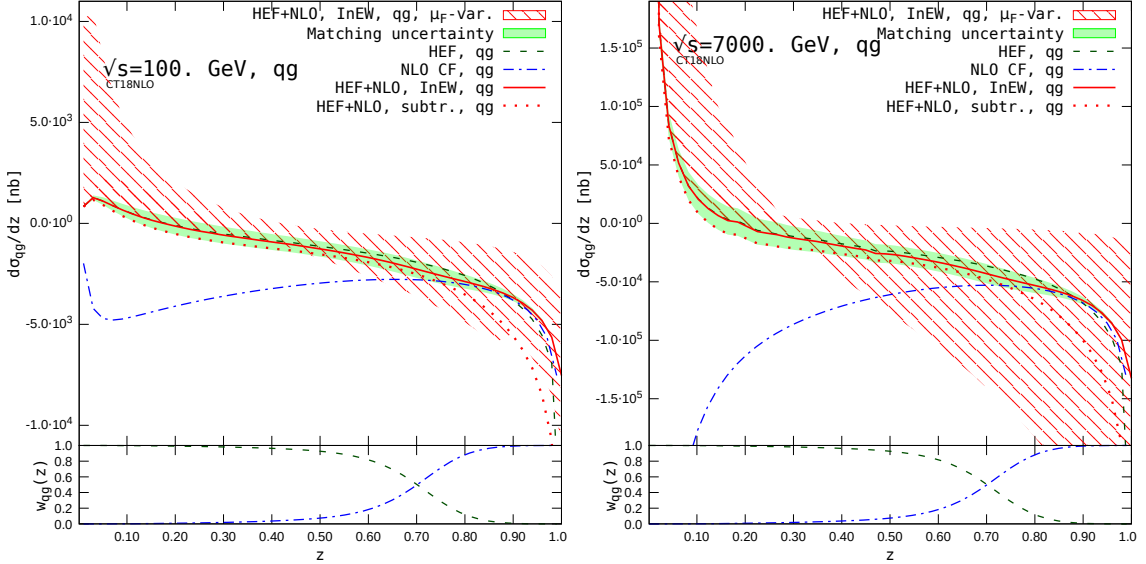


Figure 6. Matching plots for qg -channel to the $^1S_0^{[1]}$ -state hadroproduction with $M = 3$ GeV. The integrand of eqn. (3.1), i.e. subtractive matching prescription is shown for comparison by the dotted red line. The plots of InEW weights are shown in the bottom inset, while the matching uncertainty (3.4) is shown as the solid band. The LDME $\langle \mathcal{O}[^1S_0^{[1]}] \rangle$ was set to 1 GeV^3 .

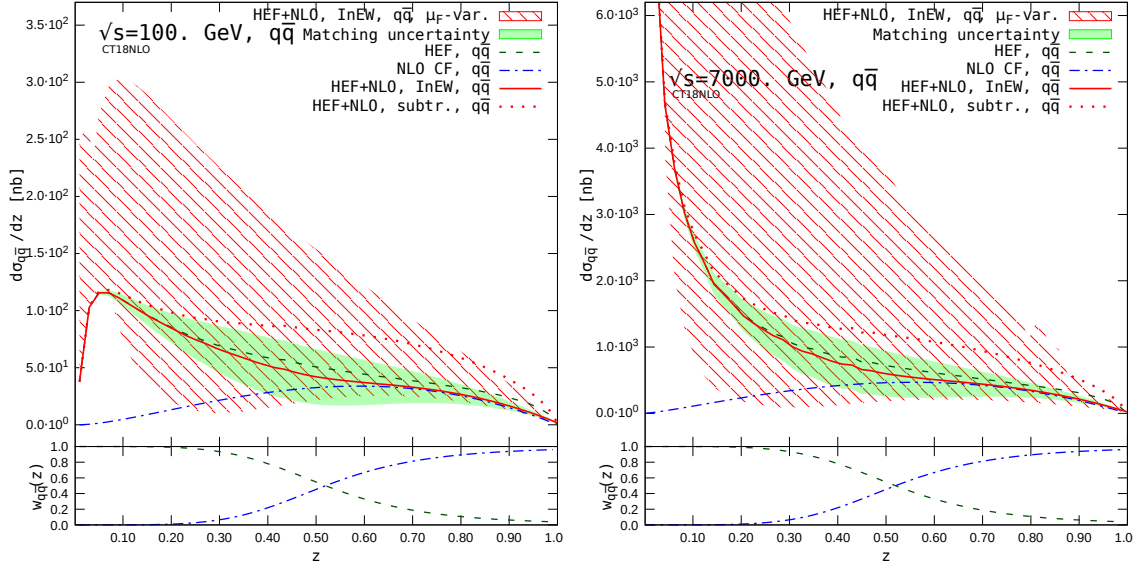


Figure 7. Matching plots for $q\bar{q}$ -channel to the $^1S_0^{[1]}$ -state hadroproduction with $M = 3$ GeV. The integrand of eqn. (3.1), i.e. subtractive matching prescription is shown for comparison by the dotted red line. The plots of InEW weights are shown in the bottom inset, while the matching uncertainty (3.4) is shown as the solid band. The LDME $\langle \mathcal{O}[^1S_0^{[1]}] \rangle$ was set to 1 GeV^3 .

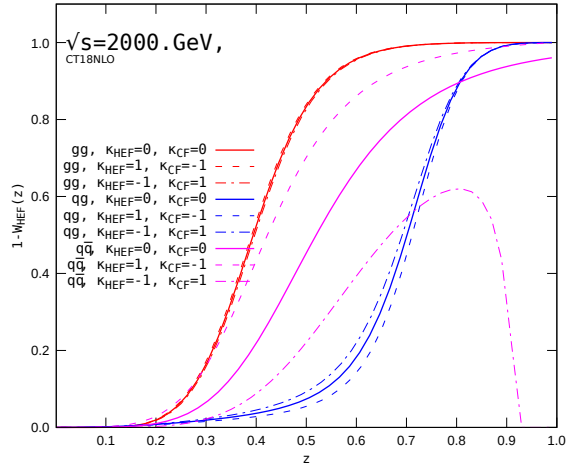


Figure 8. Dependence of the InEW weights for $\mu_F = \mu_R = M$ on the parameters κ_{CF} and κ_{HEF} .

NLO DGLAP splitting functions and thus fit seamlessly into our NLO+DLA matching scheme. The last PDF set [50] contains the NLL($\ln(1/z)$) resummation and is included in figure 9 to show that the corresponding cross section, obtained in the NLO+DLA $\ln(1/z)$ -resummation scheme, is consistent with the other results within uncertainties.

On one hand, figure 9 shows that there is a significant spread in the charmonium production cross sections at high energy, due to the PDF uncertainties at small values of x . At $\sqrt{s} = 13$ TeV, the central values of NLO+LL($\ln(1/z)$) predictions obtained with different PDFs vary as much as by factor 1.5 up and down from our default CT18NLO-based estimations. This demonstrates a potential usefulness of this observable to constrain PDFs at small x . On the other hand, the theoretical uncertainties of our predictions, dominated by the scale-variation uncertainties shown in figure 9, are still larger than the spread between central curves, so to reliably discriminate between them, the scale uncertainties have to be significantly reduced which we expected to be realised once a NLL computation is available.

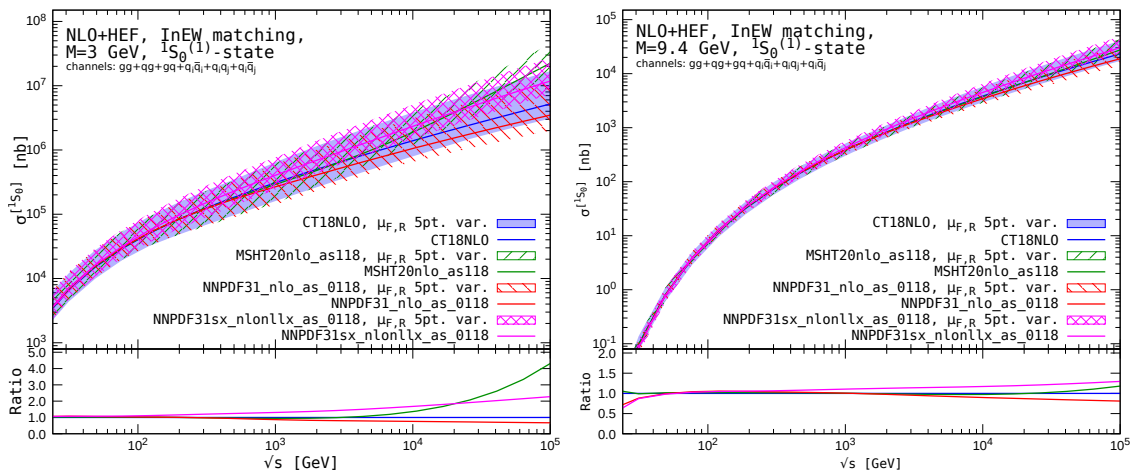


Figure 9. Dependence of the matched cross section on the choice of collinear PDF. The LDME $\langle \mathcal{O}[^1S_0^{(1)}] \rangle$ was set to 1 GeV^3 .

4 Conclusions and outlook

In the present paper, we have performed an exploratory study of the effects of High-Energy resummation on heavy-quarkonium hadroproduction cross sections. We have introduced the DLA for the resummation contributions, which is consistent with the fixed-order DGLAP evolution of PDFs and have shown that matching the NLO CF and the DL resummed HEF results solves the problem of the negative NLO CF cross sections at high energy. This opens up the possibility to use this observable to constrain PDFs at small- x , however the scale uncertainties of our predictions have to be significantly reduced. To this end, advancing such calculation to a complete NLO+NLL($\ln(1/z)$) accuracy is required, which is a work in progress.

Acknowledgments

We thank Renaud Boussarie, Francesco Hautmann and Samuel Wallon for useful discussions as well as Kate Lynch and Yelyzaveta Yedelkina for comments on the manuscript. This project has received funding from the European Union’s Horizon 2020 research and innovation programme under grant agreement STRONG–2020 No 824093 in order to contribute to the EU Virtual Access NLOACCESS (VA1-WG10) & to the Joint Research activity “Fixed Target Experiments at the LHC” (JRA2). This project has also received funding from the Agence Nationale de la Recherche (ANR) via the grant ANR-20-CE31-0015 (“PrecisOnium”) and via the IDEX Paris-Saclay “Investissements d’Avenir” (ANR-11-IDEX-0003-01) through the GLUODYNAMICS project funded by the “P2IO LabEx (ANR-10-LABX-0038)”. This work was also partly supported by the French CNRS via the GDR QCD, via the IN2P3 project GLUE@NLO, via the Franco-Polish EIA (Gluegraph). M.A.O.’s work was partly supported by the ERC grant 637019 “MathAm”.

A Numerics in z -space

A.1 Method 1: regularised resummation factor

This method is based on the following regularised form of the resummation factor, where the small- \mathbf{q}_T oscillations are replaced by a constant in \mathbf{q}_T -behaviour for $\mathbf{q}_T^2 < \mathbf{q}_{T0}^2$ in such a way that the normalisation condition (2.31) still holds exactly:

$$\tilde{c}_{gg}^{\text{DLA}}(z, \mathbf{q}_T^2, \mu_F^2) = \begin{cases} \frac{1}{\mathbf{q}_{T0}^2} \left[\delta(1-z) - \mathcal{F}\left(\frac{\mathbf{q}_{T0}^2}{\mu_F^2}, z\right) \right], & \text{if } \mathbf{q}_T^2 < \mathbf{q}_{T0}^2, \\ \mathcal{C}_{gg}^{\text{DLA}}(z, \mathbf{q}_T^2, \mu_F^2), & \text{if } \mathbf{q}_T^2 > \mathbf{q}_{T0}^2, \end{cases} \quad (\text{A.1})$$

where

$$\mathcal{F}\left(\frac{\mathbf{q}_{T0}^2}{\mu_F^2}, z\right) = \int_0^{L_{\max}} dL J_0\left(2\sqrt{L \ln \frac{1}{z}}\right) = L_{\max} {}_0\tilde{F}_1\left(2, -L_{\max} \ln \frac{1}{z}\right), \quad (\text{A.2})$$

with $L_{\max} = \hat{\alpha}_s \ln(\mathbf{q}_{T0}^2/\mu_F^2)$ and ${}_0\tilde{F}_1$, which is the regularised confluent hypergeometric function. In the $\mathbf{q}_{T0}^2 \rightarrow 0$ limit, the function \mathcal{F} turns into $\delta(1-z)$ but this limit is approached very slowly. So, for all reasonable values of $|\mathbf{q}_{T0}|$, even as small as 10^{-3} GeV, the function (A.2) is still rather smoothly dependent on z and does not cause any numerical problems. For the quark-induced channel, the regularised resummation factor:

$$\tilde{c}_{gq}^{\text{DLA}}(z, \mathbf{q}_T^2, \mu_F^2) = \frac{C_F}{C_A} \begin{cases} -\frac{1}{\mathbf{q}_{T0}^2} \mathcal{F}\left(\frac{\mathbf{q}_{T0}^2}{\mu_F^2}, z\right), & \text{if } \mathbf{q}_T^2 < \mathbf{q}_{T0}^2, \\ \mathcal{C}_{gq}^{\text{DLA}}(z, \mathbf{q}_T^2, \mu_F^2), & \text{if } \mathbf{q}_T^2 > \mathbf{q}_{T0}^2, \end{cases} \quad (\text{A.3})$$

satisfies the normalisation condition (2.32).

After substituting the regularised resummation factors (A.1) or (A.3) into eqn. (2.6), one splits the $\mathbf{q}_{T1,2}^2$ -integrations into regions with $\mathbf{q}_{T1,2}^2 < \mathbf{q}_{T0}^2$ and $\mathbf{q}_{T1,2}^2 > \mathbf{q}_{T0}^2$. If, for example $\mathbf{q}_{T1}^2 < \mathbf{q}_{T0}^2$, then this transverse momentum can be neglected in all the rest of the integrand in eqn. (2.6) because the dependence of the HEF coefficient function as well as the dependence of the factor $1/M_T^4$ on \mathbf{q}_{T1}^2 is smooth. This approximation allows one to

trivially integrate out \mathbf{q}_{T1}^2 in the region $\mathbf{q}_{T1}^2 < \mathbf{q}_{T0}^2$ introducing the error which scales as $\mathcal{O}(\mathbf{q}_{T0}^2/M^2)$ and can be made negligible by choosing a reasonably small value of \mathbf{q}_{T0}^2 . In the region $\mathbf{q}_{T1}^2 > \mathbf{q}_{T0}^2$ no approximations are made. The \mathbf{q}_{T2}^2 -integration can be decomposed in the same manner and the region where both $\mathbf{q}_{T1}^2 < \mathbf{q}_{T0}^2$ and $\mathbf{q}_{T2}^2 < \mathbf{q}_{T0}^2$ produces the LO CF term in eqn. (2.7), while the LO-subtracted partonic cross section in the method under consideration is decomposed as follows:

$$\check{\sigma}_{gg}^{[m], \text{HEF}} = \check{\sigma}_{2\text{UI}}^{[m]} + \check{\sigma}_{2\text{F}}^{[m]} + 2 \left[\check{\sigma}_{1\text{UI-C}}^{[m]} - \check{\sigma}_{1\text{UI-CF}}^{[m]} - \check{\sigma}_{\text{F}}^{[m]} \right], \quad (\text{A.4})$$

where the separate contributions depend on the value of the cut \mathbf{q}_{T0} but this dependence should cancel in their sum for sufficiently small $\mathbf{q}_{T0}^2 \ll M^2$. For the quark-induced channels, the resummed partonic coefficient can be calculated in terms of the same contributions as:

$$\hat{\sigma}_{gq}^{[m], \text{HEF}} = \frac{C_F}{C_A} \left[\check{\sigma}_{2\text{UI}}^{[m]} + \check{\sigma}_{2\text{F}}^{[m]} + \check{\sigma}_{1\text{UI-C}}^{[m]} - 2\check{\sigma}_{1\text{UI-CF}}^{[m]} - \check{\sigma}_{\text{F}}^{[m]} \right], \quad (\text{A.5})$$

$$\hat{\sigma}_{q\bar{q}}^{[m], \text{HEF}} = \left(\frac{C_F}{C_A} \right)^2 \left[\check{\sigma}_{2\text{UI}}^{[m]} + \check{\sigma}_{2\text{F}}^{[m]} - 2\check{\sigma}_{1\text{UI-CF}}^{[m]} \right]. \quad (\text{A.6})$$

The *doubly-unintegrated* contribution, $\check{\sigma}_{2\text{UI}}^{[m]}$, entering eqns. (A.4), (A.5) and (A.6) is just eqn. (2.6) with both $\mathbf{q}_{T1,2}^2 > \mathbf{q}_{T0}^2$ and the resummation factor (2.30). Other contributions are calculated as follows:

$$\begin{aligned} \check{\sigma}_{1\text{UI-CF}}^{[m]} &= \int_{-\infty}^{+\infty} d\eta \int_{\mathbf{q}_{T0}^2}^{\infty} d\mathbf{q}_{T1}^2 \mathcal{C}_{gg}^{\text{DLA}} \left(\sqrt{z} \frac{M_{T1}}{M} e^\eta, \mathbf{q}_{T1}^2, \mu_F, \mu_R \right) \\ &\quad \times \mathcal{F} \left(\frac{\mathbf{q}_{T0}^2}{\mu_F^2}, \sqrt{z} \frac{M_{T1}}{M} e^{-\eta} \right) \int_0^{2\pi} \frac{d\phi}{2} \frac{H(\mathbf{q}_{T1}^2, 0, \phi)}{M_{T1}^4}, \end{aligned} \quad (\text{A.7})$$

$$\check{\sigma}_{1\text{UI-C}}^{[m]} = \int_{\mathbf{q}_{T0}^2}^{\infty} d\mathbf{q}_{T1}^2 \mathcal{C}_{gg}^{\text{DLA}} \left(z \frac{M_{T1}^2}{M^2}, \mathbf{q}_{T1}^2, \mu_F, \mu_R \right) \int_0^{2\pi} \frac{d\phi}{2} \frac{H(\mathbf{q}_{T1}^2, 0, \phi)}{M_{T1}^4}, \quad (\text{A.8})$$

$$\check{\sigma}_{2\text{F}}^{[m]} = \int_{-\infty}^{\infty} d\eta \mathcal{F} \left(\frac{\mathbf{q}_{T0}^2}{\mu_F^2}, \sqrt{z} e^\eta \right) \mathcal{F} \left(\frac{\mathbf{q}_{T0}^2}{\mu_F^2}, \sqrt{z} e^{-\eta} \right) \int_0^{2\pi} \frac{d\phi}{2} \frac{H(0, 0, \phi)}{M^4}, \quad (\text{A.9})$$

$$\check{\sigma}_{\text{F}}^{[m]} = \mathcal{F} \left(\frac{\mathbf{q}_{T0}^2}{\mu_F^2}, z \right) \int_0^{2\pi} \frac{d\phi}{2} \frac{H(0, 0, \phi)}{M^4}, \quad (\text{A.10})$$

where $M_{T1}^2 = M^2 + \mathbf{q}_{T1}^2$.

A.2 Method 2: small- \mathbf{q}_T subtraction

The approach described in this section has been inspired by the treatment of the same problem in the ref. [44]. The method relies on the same kind of decomposition of the transverse-momentum dependence of the integrand as in eqn. (2.39), but now we perform it to isolate the LO contribution, using the normalisation condition (2.31). To save space,

let us introduce the short-hand notation for the integrand of eqn. (2.6) :

$$\begin{aligned} \mathcal{J}(\xi_1, \xi_2) &= \mathcal{C}_{gg} \left(\sqrt{z} \frac{M_T(\xi_1, \xi_2)}{M} e^\eta, \mathbf{q}_{T1}^2, \mu_F, \mu_R \right) \mathcal{C}_{gg} \left(\sqrt{z} \frac{M_T(\xi_1, \xi_2)}{M} e^{-\eta}, \mathbf{q}_{T2}^2, \mu_F, \mu_R \right) \\ &\times \frac{H(\xi_1^2 \mathbf{q}_{T1}^2, \xi_2^2 \mathbf{q}_{T2}^2, \phi)}{M_T^4(\xi_1, \xi_2)}, \end{aligned} \quad (\text{A.11})$$

where $M_T^2(\xi_1, \xi_2) = M^2 + (\xi_1 \mathbf{q}_{T1} + \xi_2 \mathbf{q}_{T2})^2$ and variables $\xi_{1,2} = \{0, 1\}$ are introduced for us to be able to turn on and off the ‘‘smooth part’’ of the dependence of the integrand on transverse momenta, while the dependence of \mathcal{J} on $\mathbf{q}_{T1,2}^2$, ϕ and η is implicit. Similarly to eqn. (2.39) we decompose

$$\mathcal{J}(1, 1) = \mathcal{J}_1 + \mathcal{J}_2 + \mathcal{J}_3 + \mathcal{J}(0, 0) \theta(\mu_F^2 - \mathbf{q}_{T1}^2) \theta(\mu_F^2 - \mathbf{q}_{T2}^2),$$

where the last term of this decomposition, when substituted to eqn. (2.6) gives us $\sigma_{\text{LO}}^{[m]} \delta(1-z)$ due to normalisation condition (2.31), while the terms $\mathcal{J}_{1,2,3}$ are:

$$\begin{aligned} \mathcal{J}_1 &= \mathcal{J}(1, 1) - \mathcal{J}(0, 1) \theta(\mu_F^2 - \mathbf{q}_{T1}^2) \\ &\quad - \mathcal{J}(1, 0) \theta(\mu_F^2 - \mathbf{q}_{T2}^2) + \mathcal{J}(0, 0) \theta(\mu_F^2 - \mathbf{q}_{T1}^2) \theta(\mu_F^2 - \mathbf{q}_{T2}^2), \\ \mathcal{J}_2 &= \left[\mathcal{J}(1, 0) - \mathcal{J}(0, 0) \theta(\mu_F^2 - \mathbf{q}_{T1}^2) \right] \theta(\mu_F^2 - \mathbf{q}_{T2}^2), \\ \mathcal{J}_3 &= \left[\mathcal{J}(0, 1) - \mathcal{J}(0, 0) \theta(\mu_F^2 - \mathbf{q}_{T2}^2) \right] \theta(\mu_F^2 - \mathbf{q}_{T1}^2). \end{aligned}$$

Using these expressions, the *doubly-unintegrated* contribution $\check{\sigma}_{2\text{UI-S}}^{[m]}$ in this method is defined as eqn. (2.6) with integrand \mathcal{J}_1 and without any low- $\mathbf{q}_{T1,2}$ cuts. The *single-unintegrated* contribution is obtained by substituting \mathcal{J}_2 into eqn. (2.6) and integrating out \mathbf{q}_{T2}^2 via eqn. (2.31):

$$\begin{aligned} \check{\sigma}_{1\text{UI-S}}^{[m]} &= \int_0^\infty d\mathbf{q}_{T1}^2 \int_0^{2\pi} \frac{d\phi}{2} \left[\mathcal{C}_{gg} \left(z \frac{M_{T1}^2}{M^2}, \mathbf{q}_{T1}^2, \mu_F^2, \mu_R^2 \right) \frac{H(\mathbf{q}_{T1}^2, 0, \phi)}{M_{T1}^4} \right. \\ &\quad \left. - \mathcal{C}_{gg} \left(z, \mathbf{q}_{T1}^2, \mu_F^2, \mu_R^2 \right) \frac{H(0, 0, \phi)}{M^4} \theta(\mu_F^2 - \mathbf{q}_{T1}^2) \right]. \end{aligned} \quad (\text{A.12})$$

The LO subtracted resummed cross section for the gg channel is calculated as:

$$\check{\sigma}_{gg}^{[m], \text{HEF}} = \check{\sigma}_{2\text{UI-S}}^{[m]} + 2\check{\sigma}_{1\text{UI-S}}^{[m]}, \quad (\text{A.13})$$

while, for the quark-induced channels, one has:

$$\hat{\sigma}_{gq}^{[m], \text{HEF}} = \frac{C_F}{C_A} \left[\check{\sigma}_{2\text{UI-S}}^{[m]} + \check{\sigma}_{1\text{UI-S}}^{[m]} \right], \quad (\text{A.14})$$

$$\hat{\sigma}_{q\bar{q}}^{[m], \text{HEF}} = \left(\frac{C_F}{C_A} \right)^2 \check{\sigma}_{2\text{UI-S}}^{[m]}. \quad (\text{A.15})$$

For the DLA resummation factor, the numerical results obtained in both methods agree within the integration accuracy. However, the subtraction method allows one to work with

resummation factor given in the numerical form. The only requirement is that it should satisfy the normalisation condition (2.31), which is true for example for the resummation factor (2.18) with full LL($\ln(1/z)$) anomalous dimension, obtained as numerical solution of eqn. (2.19), but with $R(\gamma) = 1$, as discussed in Appendix B, or for the Gaussian-smeared resummation factor discussed in Appendix C.

B Effects of the anomalous dimension beyond LO

In this appendix, we study the effects of terms beyond LO in α_s in the anomalous dimension (2.20) on the resummed cross section, while still omitting the scheme-transformation factor $R(\gamma)$ from the eqn. (2.18). We have obtained the numerical solution of eqn. (2.19), which in terms of the variable $\rho = N/\hat{\alpha}_s$ has the form:

$$\chi(\gamma_{gg}(\rho)) = \rho. \quad (\text{B.1})$$

This equation has already been studied numerically in refs. [70, 75]. The perturbative branch of the solution has a cut-discontinuity depicted in the figure 10, and inverse Mellin transform integral (2.29) can be written as an integral over the contour in ρ -plane which should avoid crossing this cut. Our numerical results for the real and imaginary parts of the solution agree with results of ref. [70] and are also shown on figure 10.

Plots of the resummation factor resulting from the numerical inverse Mellin transform are shown on figure 11. At moderately small values of z , it is close to the DLA, but at smaller values of z it deviates from DLA and the most numerically important region of $\mathbf{q}_T^2 \sim 1 \text{ GeV}^2$ features a significant peak in the negative direction.

On figure 12, the \sqrt{s} -dependence of the HEF-resummed part of the total cross section of production of the $Q\bar{Q}[^1S_0^{(1)}]$ state in the gg channel is plotted. The central lines as well as uncertainty bands resulting from the variation of μ_F by a factor of 2 above and below the default value $\mu_F = M$ are presented. Two approximations for the resummation factor are compared on figure 12: the DLA, introduced in the section 2.3, and the approximation described above in this appendix, which includes effects beyond LO in $\gamma_{gg}(N, \alpha_s)$. The LO CF central curve and the μ_F uncertainty is also shown on figure 12 for comparison. One can see that, while DLA significantly reduces the scale uncertainty in comparison to the LO CF result, the inclusion of higher-order corrections to $\gamma_{gg}(N, \alpha_s)$ blows up the scale uncertainty at high energies so much that, for $\sqrt{s} > 4 \text{ TeV}$ (left panel of the figure 12) or $\sqrt{s} > 7 \text{ TeV}$ (right panel of the figure 12), the resummed part of cross section can become negative.

This catastrophic factorisation-scale uncertainty is a consequence of the mismatch between the μ_F -dependence of the resummation factor and one of the collinear PDFs used. For the left plot on figure 12, we have employed the central eigenset of the NNPDF31_nlo_as_0118 [73] PDFs and, in the right panel, the NLL($\ln(1/z)$)-resummed version of the NNPDF31 PDFs has been used [50]. Figure 12 serves as a numerical illustration of our statement in section 2.3 that one should not increase the accuracy of the resummation factors in HEF beyond DLA if collinear PDFs result from a fixed-order DGLAP evolution, as in the left plot of figure 12. In the case of the NLL($\ln(1/z)$)-resummed PDFs (right

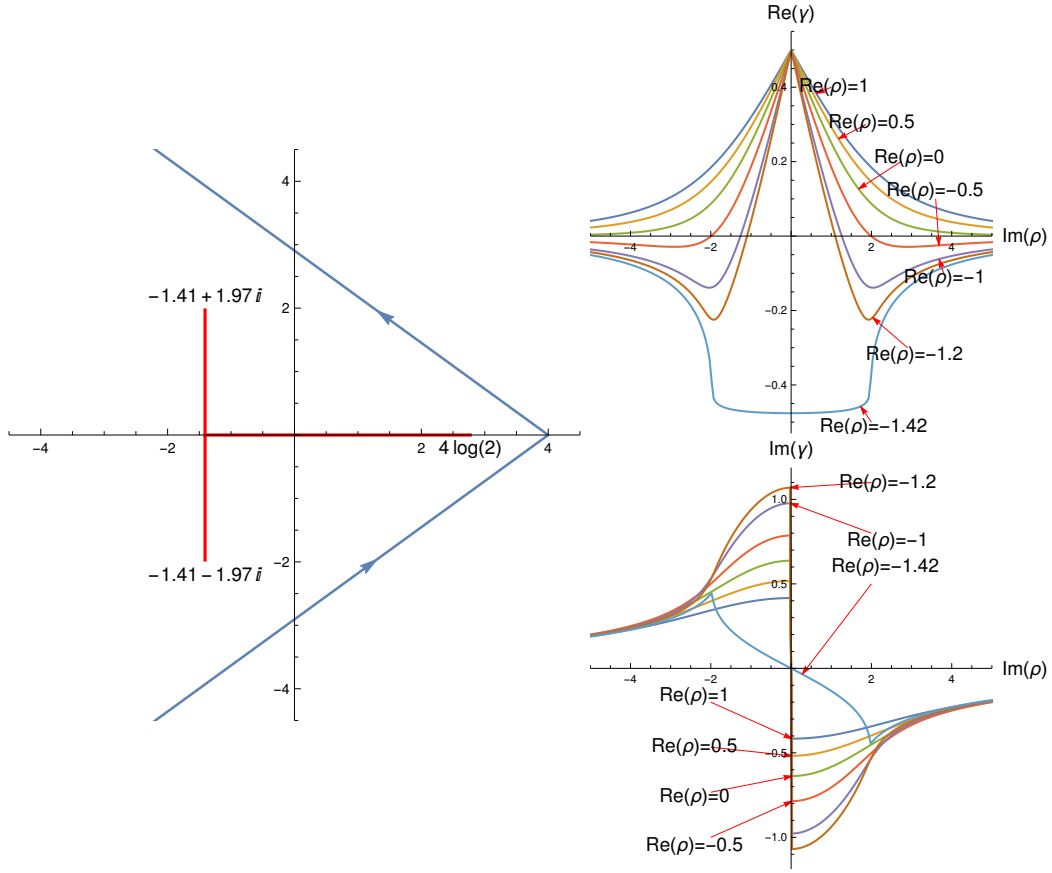


Figure 10. Left panel: branch cut discontinuity of the function $\gamma_{gg}(\rho)$ and the integration contour of the inverse Mellin transform in the ρ -plane. Right panel: real and imaginary parts of $\gamma_{gg}(\rho)$ as functions of $\text{Im} \rho$ at fixed $\text{Re} \rho = 1, 0.5, 0, -0.5, -1, -1.2, -1.42$. To be compared with the plots in the figure 1 of the ref. [70].

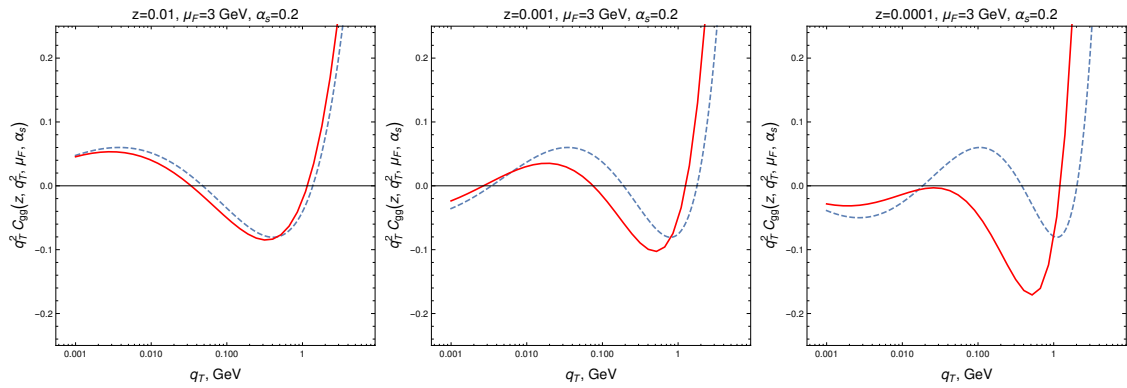


Figure 11. Resummation factor C_{gg} as a function of $|q_T|$ for several values of z . The DLA result is plotted by the dashed curve and numerical result with $\text{LL}(\ln(1/z))$ anomalous dimension, obtained as a solution of eqn. (2.19) is plotted by the solid curve.

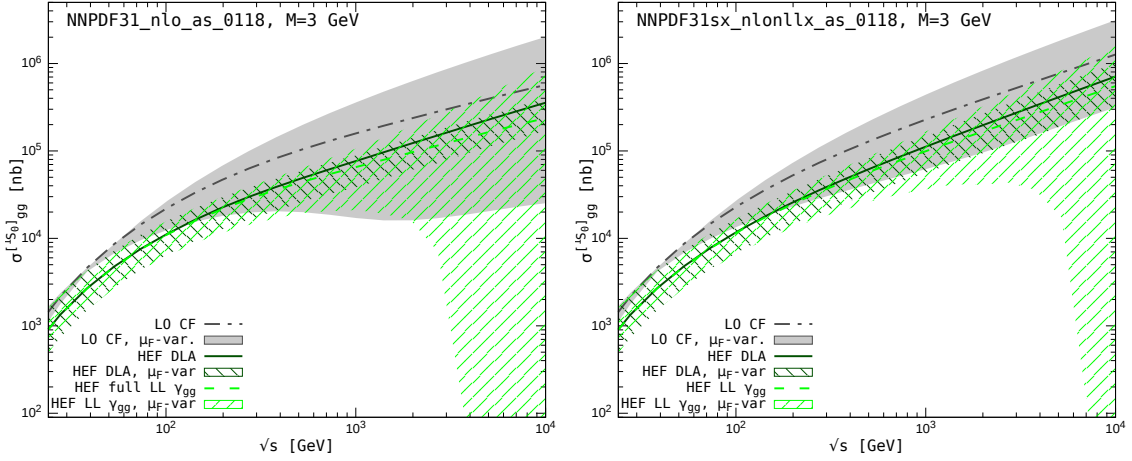


Figure 12. Energy dependence of the HEF resummed part of the cross section (LO CF included) in the gg channel: the DLA result and its μ_F -variation are plotted as solid line and left-shaded band, dashed line and right-shaded μ_F -variation band correspond to the calculation using the full numerical solution of eqn. (2.19) for $\gamma_{gg}(N, \alpha_s)$. For comparison, the LO CF cross section together with its μ_F -variation is shown by the dash-dotted line and the corresponding solid band. The gluon PDFs used are NNPDF31_nlo_as_0118 [73](left panel) and NNPDF31sx_nlonllx_as_0118 [50](right panel). The LDME $\langle \mathcal{O}[^1S_0^{(1)}] \rangle$ was set to 1 GeV^3 .

panel of figure 12), the addition of the full LL($\ln(1/z)$) correction to γ_{gg} is also not justified because in this case the formal perturbative accuracy of the PDFs is greater than that of the resummation factor and the NLL resummed version γ_{gg} is significantly [50, 76] different from the full LL($\ln(1/z)$)-resummed one, so even in this case we have a mismatch of the μ_F -dependence between the PDFs and the resummation factor.

C Higher-twist effects

It may be argued that the oscillatory behaviour of the resummation factors at $\mathbf{q}_T^2 \ll 1 \text{ GeV}^2$, depicted on figure 11, is un-physical and that in this domain the resummation factor is dominated by non-perturbative effects. In this context, one would like to understand how much the total cross section depends on the detailed behaviour of the resummation factor at small values of \mathbf{q}_T^2 . As a toy model to study this question, we have performed a convolution of the DLA resummation factor (2.28) with Gaussian of the width σ_T in transverse momentum which can be done analytically with the Mellin-space result (2.28):

$$\begin{aligned}
 \mathcal{C}_{gg}^{\text{DLA},\sigma}(N, \mathbf{q}_T^2, \mu_F, \mu_R) &= \int \frac{d^2 \mathbf{k}_T}{\pi \sigma_T^2} \exp \left[-\frac{\mathbf{k}_T^2}{\sigma_T^2} \right] \mathcal{C}_{gg}^{\text{DLA}}(N, (\mathbf{q}_T + \mathbf{k}_T)^2, \mu_F, \mu_R) \\
 &= \frac{1}{\sigma_T^2} \left(\frac{\sigma_T^2}{\mu_F^2} \right)^{\gamma_N} e^{-\frac{\mathbf{q}_T^2}{\sigma_T^2}} {}_1F_1 \left(\gamma_N, 1, \frac{\mathbf{q}_T^2}{\sigma_T^2} \right), \quad (\text{C.1})
 \end{aligned}$$

and then converted it to the z -space numerically. Eqn. (C.1) still satisfies the normalisation condition (2.31) up to corrections suppressed as $e^{-\mu_F^2/\sigma_T^2}$, so the method from the

section A.2 can be used to calculate the cross section if $\sigma_T \lesssim 1$ GeV. Several plots of the $|\mathbf{q}_T|$ -dependence of the smeared resummation factor (C.1), transformed numerically to the z -space are presented in the left panel of figure 13.

In the right panel of figure 13, the ratio of the matched cross section obtained with the Gaussian-smeared resummation factor to the cross section without \mathbf{k}_T -smearing is plotted as a function of \sqrt{s} for $\sigma_T = 0.5$ and 1 GeV. The results with $\sigma_T = 0.5$ and 1 GeV differ from the matched cross section calculated without a Gaussian by at most ten percent for $\mu_F = 0.5M$ and $2M$, while the results at the default scale are even closer.

From the detailed consideration of the small- \mathbf{q}_T subtraction method, described in section A.2, one can see that the effect of the \mathbf{k}_T -smearing on the total cross section is suppressed as $\mathcal{O}(\sigma_T^2/M^2) \sim \mathcal{O}(\Lambda_{\text{QCD}}^2/M^2)$ if $\sigma_T \sim \Lambda_{\text{QCD}}$. In other words, these effect follow a subleading power in our hard scale M ; it is a *higher-twist effect*.

The width of the “intrinsic” \mathbf{k}_T -distribution is expected to be increasing with energy, due to increasing saturation scale (see e.g. ref. [77] and references therein), so that, at high enough energies, the twist expansion will completely break down due to the effect discussed above. However, as one can see from figure 13 this effects are unlikely to be the main source of uncertainty in our calculation at LHC energies and even beyond.

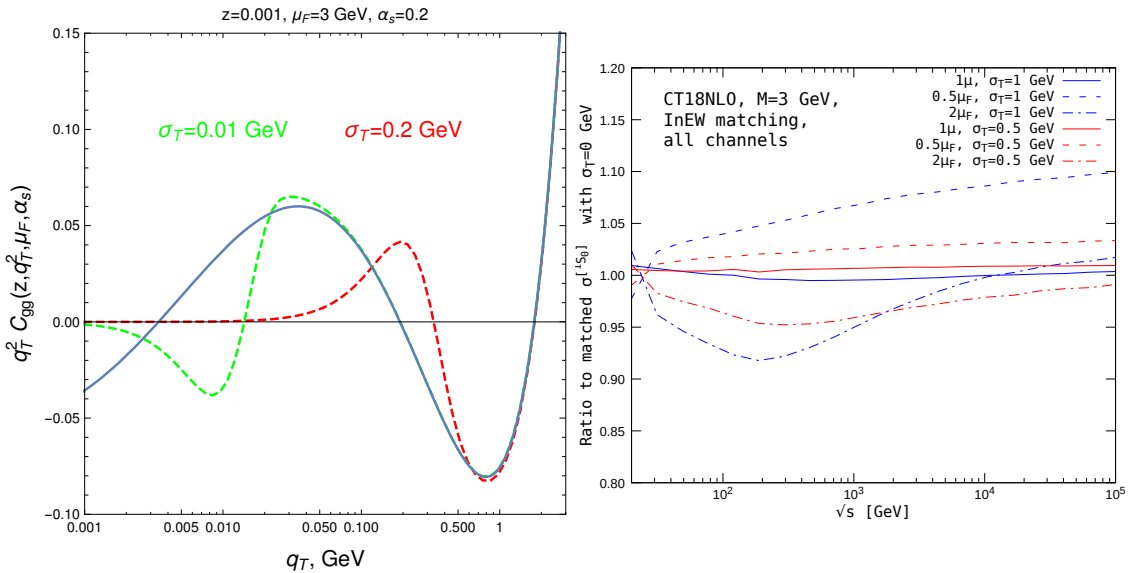


Figure 13. **Left panel:** the q_T -dependence of the Gaussian smeared DLA resummation factor for two values of σ_T (dashed curves). The DLA resummation factor without smearing (2.30) is shown by solid curve for comparison. **Right panel:** the energy-dependence of the ratio of the matched cross section obtained in the DLA with Gaussian smearing with $\sigma_T = 0.5$ and 1 GeV to the result without smearing and its μ_F -scale variation.

References

- [1] E. Chapon et al., *Perspectives for quarkonium studies at the high-luminosity LHC*, [2012.14161](https://arxiv.org/abs/2012.14161).

- [2] A. Arbuzov et al., *On the physics potential to study the gluon content of proton and deuteron at NICA SPD*, *Prog. Part. Nucl. Phys.* **119** (2021) 103858 [[2011.15005](#)].
- [3] J.-P. Lansberg, *New Observables in Inclusive Production of Quarkonia*, *Phys. Rept.* **889** (2020) 1 [[1903.09185](#)].
- [4] N. Brambilla et al., *QCD and Strongly Coupled Gauge Theories: Challenges and Perspectives*, *Eur. Phys. J. C* **74** (2014) 2981 [[1404.3723](#)].
- [5] N. Brambilla et al., *Heavy Quarkonium: Progress, Puzzles, and Opportunities*, *Eur. Phys. J. C* **71** (2011) 1534 [[1010.5827](#)].
- [6] G.T. Bodwin, E. Braaten and G.P. Lepage, *Rigorous QCD analysis of inclusive annihilation and production of heavy quarkonium*, *Phys. Rev. D* **51** (1995) 1125 [[hep-ph/9407339](#)].
- [7] M. Butenschoen and B.A. Kniehl, *Reconciling J/ψ production at HERA, RHIC, Tevatron, and LHC with NRQCD factorization at next-to-leading order*, *Phys. Rev. Lett.* **106** (2011) 022003 [[1009.5662](#)].
- [8] M. Butenschoen and B.A. Kniehl, *World data of J/ψ production consolidate NRQCD factorization at NLO*, *Phys. Rev. D* **84** (2011) 051501 [[1105.0820](#)].
- [9] M. Butenschoen and B.A. Kniehl, *J/ψ polarization at Tevatron and LHC: Nonrelativistic-QCD factorization at the crossroads*, *Phys. Rev. Lett.* **108** (2012) 172002 [[1201.1872](#)].
- [10] M. Butenschoen and B.A. Kniehl, *Next-to-leading-order tests of NRQCD factorization with J/ψ yield and polarization*, *Mod. Phys. Lett. A* **28** (2013) 1350027 [[1212.2037](#)].
- [11] K.-T. Chao, Y.-Q. Ma, H.-S. Shao, K. Wang and Y.-J. Zhang, *J/ψ Polarization at Hadron Colliders in Nonrelativistic QCD*, *Phys. Rev. Lett.* **108** (2012) 242004 [[1201.2675](#)].
- [12] B. Gong, L.-P. Wan, J.-X. Wang and H.-F. Zhang, *Polarization for Prompt J/ψ and $\psi(2s)$ Production at the Tevatron and LHC*, *Phys. Rev. Lett.* **110** (2013) 042002 [[1205.6682](#)].
- [13] G.T. Bodwin, H.S. Chung, U.-R. Kim and J. Lee, *Fragmentation contributions to J/ψ production at the Tevatron and the LHC*, *Phys. Rev. Lett.* **113** (2014) 022001 [[1403.3612](#)].
- [14] B. Gong, J.-X. Wang and H.-F. Zhang, *QCD corrections to Υ production via color-octet states at the Tevatron and LHC*, *Phys. Rev. D* **83** (2011) 114021 [[1009.3839](#)].
- [15] K. Wang, Y.-Q. Ma and K.-T. Chao, *$\Upsilon(1S)$ prompt production at the Tevatron and LHC in nonrelativistic QCD*, *Phys. Rev. D* **85** (2012) 114003 [[1202.6012](#)].
- [16] B. Gong, L.-P. Wan, J.-X. Wang and H.-F. Zhang, *Complete next-to-leading-order study on the yield and polarization of $\Upsilon(1S, 2S, 3S)$ at the Tevatron and LHC*, *Phys. Rev. Lett.* **112** (2014) 032001 [[1305.0748](#)].
- [17] M. Butenschoen, Z.-G. He and B.A. Kniehl, *η_c production at the LHC challenges nonrelativistic-QCD factorization*, *Phys. Rev. Lett.* **114** (2015) 092004 [[1411.5287](#)].
- [18] V.D. Barger, W.-Y. Keung and R.J.N. Phillips, *On ψ and Upsilon Production via Gluons*, *Phys. Lett. B* **91** (1980) 253.
- [19] V.D. Barger, W.-Y. Keung and R.J.N. Phillips, *Hadroproduction of ψ and Υ* , *Z. Phys. C* **6** (1980) 169.
- [20] R. Gavai, D. Kharzeev, H. Satz, G.A. Schuler, K. Sridhar and R. Vogt, *Quarkonium production in hadronic collisions*, *Int. J. Mod. Phys. A* **10** (1995) 3043 [[hep-ph/9502270](#)].

- [21] Y.-Q. Ma and R. Vogt, *Quarkonium Production in an Improved Color Evaporation Model*, *Phys. Rev. D* **94** (2016) 114029 [[1609.06042](#)].
- [22] J.-P. Lansberg, H.-S. Shao, N. Yamanaka, Y.-J. Zhang and C. Noûs, *Complete NLO QCD study of single- and double-quarkonium hadroproduction in the colour-evaporation model at the Tevatron and the LHC*, *Phys. Lett. B* **807** (2020) 135559 [[2004.14345](#)].
- [23] N. Brambilla, H.S. Chung and A. Vairo, *Inclusive production of heavy quarkonia in pNRQCD*, *JHEP* **09** (2021) 032 [[2106.09417](#)].
- [24] Y.-Q. Ma and K.-T. Chao, *New factorization theory for heavy quarkonium production and decay*, *Phys. Rev. D* **100** (2019) 094007 [[1703.08402](#)].
- [25] R. Li, Y. Feng and Y.-Q. Ma, *Exclusive quarkonium production or decay in soft gluon factorization*, *JHEP* **05** (2020) 009 [[1911.05886](#)].
- [26] A.-P. Chen and Y.-Q. Ma, *Theory for quarkonium: from NRQCD factorization to soft gluon factorization*, *Chin. Phys. C* **45** (2021) 013118 [[2005.08786](#)].
- [27] Z.-B. Kang, J.-W. Qiu and G. Sterman, *Heavy quarkonium production and polarization*, *Phys. Rev. Lett.* **108** (2012) 102002 [[1109.1520](#)].
- [28] J.H. Kuhn and E. Mirkes, *QCD corrections to toponium production at hadron colliders*, *Phys. Rev. D* **48** (1993) 179 [[hep-ph/9301204](#)].
- [29] A. Petrelli, M. Cacciari, M. Greco, F. Maltoni and M.L. Mangano, *NLO production and decay of quarkonium*, *Nucl. Phys. B* **514** (1998) 245 [[hep-ph/9707223](#)].
- [30] J.-P. Lansberg and M.A. Ozcelik, *Curing the unphysical behaviour of NLO quarkonium production at the LHC and its relevance to constrain the gluon PDF at low scales*, *Eur. Phys. J. C* **81** (2021) 497 [[2012.00702](#)].
- [31] G.A. Schuler, *Quarkonium production and decays*, 1994.
- [32] M.L. Mangano and A. Petrelli, *NLO quarkonium production in hadronic collisions*, *Int. J. Mod. Phys. A* **12** (1997) 3887 [[hep-ph/9610364](#)].
- [33] Y. Feng, J.-P. Lansberg and J.-X. Wang, *Energy dependence of direct-quarkonium production in pp collisions from fixed-target to LHC energies: complete one-loop analysis*, *Eur. Phys. J. C* **75** (2015) 313 [[1504.00317](#)].
- [34] V.N. Gribov and L.N. Lipatov, *e^+e^- -annihilation and deep-inelastic ep-scattering in perturbation theory*, *Sov. J. Nucl. Phys.* **15** (1972) 438.
- [35] Y.L. Dokshitzer, *Calculation of structure functions of deep-inelastic scattering and e^+e^- -annihilation in perturbation theory of quantum chromodynamics*, *Sov. Phys. JETP* **46** (1977) 641.
- [36] G. Altarelli and G. Parisi, *Asymptotic freedom in parton language*, *Nucl. Phys.* **B126** (1977) 298.
- [37] R.K. Ellis and D.A. Ross, *The Coupling of the QCD Pomeron in Various Semihard Processes*, *Nucl. Phys. B* **345** (1990) 79.
- [38] A.C. Serri, Y. Feng, C. Flore, J.-P. Lansberg, M.A. Ozcelik, H.-S. Shao et al., *Revisiting NLO QCD corrections to total inclusive J/psi and Upsilon photoproduction cross sections in lepton-proton collisions*, [2112.05060](#).
- [39] E.A. Kuraev, L.N. Lipatov and V.S. Fadin, *Multi - Reggeon processes in the Yang-Mills theory*, *Sov. Phys. JETP* **44** (1976) 443.

- [40] E.A. Kuraev, L.N. Lipatov and V.S. Fadin, *The Pomeron singularity in non-Abelian gauge theories*, *Sov. Phys. JETP* **45** (1977) 199.
- [41] Y.Y. Balitsky and L.N. Lipatov, *The Pomeron singularity in Quantum Chromodynamics*, *Sov. J. Nucl. Phys.* **28** (1978) 822.
- [42] S. Catani, M. Ciafaloni and F. Hautmann, *GLUON CONTRIBUTIONS TO SMALL x HEAVY FLAVOR PRODUCTION*, *Phys. Lett. B* **242** (1990) 97.
- [43] S. Catani, M. Ciafaloni and F. Hautmann, *High-energy factorization and small x heavy flavor production*, *Nucl. Phys. B* **366** (1991) 135.
- [44] J.C. Collins and R.K. Ellis, *Heavy quark production in very high-energy hadron collisions*, *Nucl. Phys.* **B360** (1991) 3.
- [45] S. Catani and F. Hautmann, *High-energy factorization and small x deep inelastic scattering beyond leading order*, *Nucl. Phys.* **B427** (1994) 475 [[hep-ph/9405388](#)].
- [46] F. Hautmann, *Heavy top limit and double logarithmic contributions to Higgs production at $m(H)^{**2} / s$ much less than 1*, *Phys. Lett.* **B535** (2002) 159 [[hep-ph/0203140](#)].
- [47] R.V. Harlander, H. Mantler, S. Marzani and K.J. Ozeren, *Higgs production in gluon fusion at next-to-next-to-leading order QCD for finite top mass*, *Eur. Phys. J. C* **66** (2010) 359 [[0912.2104](#)].
- [48] S. Marzani and R.D. Ball, *High Energy Resummation of Drell-Yan Processes*, *Nucl. Phys. B* **814** (2009) 246 [[0812.3602](#)].
- [49] G. Diana, *High-energy resummation in direct photon production*, *Nucl. Phys. B* **824** (2010) 154 [[0906.4159](#)].
- [50] R.D. Ball, V. Bertone, M. Bonvini, S. Marzani, J. Rojo and L. Rottoli, *Parton distributions with small- x resummation: evidence for BFKL dynamics in HERA data*, *Eur. Phys. J.* **C78** (2018) 321 [[1710.05935](#)].
- [51] xFITTER DEVELOPERS' TEAM collaboration, *Impact of low- x resummation on QCD analysis of HERA data*, *Eur. Phys. J.* **C78** (2018) 621 [[1802.00064](#)].
- [52] M.G. Echevarria, T. Kasemets, J.-P. Lansberg, C. Pisano and A. Signori, *Matching factorization theorems with an inverse-error weighting*, *Phys. Lett. B* **781** (2018) 161 [[1801.01480](#)].
- [53] B.L. Ioffe, V.S. Fadin and L.N. Lipatov, *Quantum Chromodynamics Perturbative and Nonperturbative Aspects*, Cambridge University Press, Cambridge (2010).
- [54] Y.V. Kovchegov and E. Levin, *Quantum Chromodynamics at High Energy*, Cambridge Monographs on Particle Physics, Nuclear Physics and Cosmology, Cambridge University Press (2012), [10.1017/CBO9781139022187](#).
- [55] V. Del Duca, *An introduction to the perturbative QCD pomeron and to jet physics at large rapidities*, *Scientifica Acta* **10** (1995) 91 [[hep-ph/9503226](#)].
- [56] J.C. Collins, *Foundations of perturbative QCD*, Cambridge University Press, Cambridge (2011).
- [57] M. Nefedov, *Sudakov resummation from the BFKL evolution*, *Phys. Rev. D* **104** (2021) 054039 [[2105.13915](#)].
- [58] M. Hentschinski, *Transverse momentum dependent gluon distribution within high energy factorization at next-to-leading order*, *Phys. Rev. D* **104** (2021) 054014 [[2107.06203](#)].

- [59] L.N. Lipatov, *Gauge invariant effective action for high-energy processes in QCD*, *Nucl. Phys.* **B452** (1995) 369.
- [60] B.A. Kniehl, V.A. Saleev and D.V. Vasin, *Bottomonium production in the Regge limit of QCD*, *Phys. Rev.* **D74** (2006) 014024 [[hep-ph/0607254](#)].
- [61] Z.-G. He, B.A. Kniehl, M.A. Nefedov and V.A. Saleev, *Double Prompt J/ψ Hadroproduction in the Parton Reggeization Approach with High-Energy Resummation*, *Phys. Rev. Lett.* **123** (2019) 162002 [[1906.08979](#)].
- [62] P. Hagler, R. Kirschner, A. Schafer, L. Szymanowski and O. Teryaev, *Heavy quark production as sensitive test for an improved description of high-energy hadron collisions*, *Phys. Rev. D* **62** (2000) 071502 [[hep-ph/0002077](#)].
- [63] P. Hagler, R. Kirschner, A. Schafer, L. Szymanowski and O.V. Teryaev, *Towards a solution of the charmonium production controversy: k^- perpendicular factorization versus color octet mechanism*, *Phys. Rev. Lett.* **86** (2001) 1446 [[hep-ph/0004263](#)].
- [64] B.A. Kniehl, D.V. Vasin and V.A. Saleev, *Charmonium production at high energy in the k_T -factorization approach*, *Phys. Rev. D* **73** (2006) 074022 [[hep-ph/0602179](#)].
- [65] T. Jaroszewicz, *Gluonic Regge Singularities and Anomalous Dimensions in QCD*, *Phys. Lett.* **116B** (1982) 291.
- [66] R. Kirschner and M. Segond, *Small x resummation in collinear factorisation*, *Eur. Phys. J. C* **68** (2010) 425 [[0910.5443](#)].
- [67] A. Vogt, S. Moch and J.A.M. Vermaseren, *The Three-loop splitting functions in QCD: The Singlet case*, *Nucl. Phys. B* **691** (2004) 129 [[hep-ph/0404111](#)].
- [68] T. Lukowski, A. Rej and V.N. Velizhanin, *Five-Loop Anomalous Dimension of Twist-Two Operators*, *Nucl. Phys. B* **831** (2010) 105 [[0912.1624](#)].
- [69] B.A. Kniehl, V.A. Saleev, A.V. Shipilova and E.V. Yatsenko, *Single jet and prompt-photon inclusive production with multi-Regge kinematics: From Tevatron to LHC*, *Phys. Rev. D* **84** (2011) 074017 [[1107.1462](#)].
- [70] J. Blumlein, *On the $k(T)$ dependent gluon density of the proton*, in *Deep inelastic scattering and QCD. Proceedings, Workshop, Paris, France, April 24-28, 1995*, pp. 265–268, 1995, <http://www-library.desy.de/cgi-bin/showprep.pl?desy95-121> [[hep-ph/9506403](#)].
- [71] T.-J. Hou et al., *New CTEQ global analysis of quantum chromodynamics with high-precision data from the LHC*, *Phys. Rev. D* **103** (2021) 014013 [[1912.10053](#)].
- [72] S. Bailey, T. Cridge, L.A. Harland-Lang, A.D. Martin and R.S. Thorne, *Parton distributions from LHC, HERA, Tevatron and fixed target data: MSHT20 PDFs*, *Eur. Phys. J. C* **81** (2021) 341 [[2012.04684](#)].
- [73] NNPDF collaboration, *Parton distributions from high-precision collider data*, *Eur. Phys. J. C* **77** (2017) 663 [[1706.00428](#)].
- [74] A. Buckley, J. Ferrando, S. Lloyd, K. Nordström, B. Page, M. Rüfenacht et al., *LHAPDF6: parton density access in the LHC precision era*, *Eur. Phys. J. C* **75** (2015) 132 [[1412.7420](#)].
- [75] R.K. Ellis, F. Hautmann and B.R. Webber, *QCD scaling violation at small x* , *Phys. Lett. B* **348** (1995) 582 [[hep-ph/9501307](#)].
- [76] G. Altarelli, R.D. Ball and S. Forte, *Resummation of singlet parton evolution at small x* , *Nucl. Phys.* **B575** (2000) 313 [[hep-ph/9911273](#)].

- [77] J.L. Albacete and C. Marquet, *Gluon saturation and initial conditions for relativistic heavy ion collisions*, *Prog. Part. Nucl. Phys.* **76** (2014) 1 [[1401.4866](#)].